Generation of hydroxyl radical during chlorination of hydroxyphenols and natural organic matter extracts

Eva M. Rodríguez [a, b], Urs von Gunten [b, c, d, *]

[a] Departamento de Ingeniería Química y Química Física, Universidad de Extremadura, Avda. Elvas s/n, 06006, Badajoz, Spain
[b] School of Architecture, Civil and Environmental Engineering (ENAC), Ecole Polytechnique Fédérale de Lausanne (EPFL), CH-1015, Lausanne, Switzerland
[c] Eawag, Swiss Federal Institute of Aquatic Science and Technology, CH-8600, Dübendorf, Switzerland
[d] Swiss Federal Institute of Technology, Institute of Biogeochemistry and Pollutant Dynamics (IBP), Department of Environment Systems (D-USYS), ETH Zurich, Universitätsstrasse 16, CH-8092, Zürich, Switzerland

ARTICLE INFO

ABSTRACT

The generation of hydroxyl radicals ($^\bullet$OH) during the chlorination of air saturated solutions of different hydroxyphenols (hydroquinone, resorcinol, catechol, gallic and tannic acids) at pH 7 has been determined by the formation of phenol (in presence of benzene in excess) or 2-hydroxyterephthalic acid (in presence of terephthalic acid). Formation of $^\bullet$OH was only detected during the chlorination of o- or p-hydroxyphenols, compounds that react with chlorine by electron transfer forming the corresponding semiquinones/quinones. In aerated solutions, oxygen is reduced by the semiquinone to the superoxide radical, $O_2^{\bullet-}$, which reacts with HOCl to $^\bullet$OH. Compared to the studied o-hydroxyphenols, the lower reactivity of hydroquinone towards chlorine favours the reaction between chlorine and $O_2^{\bullet-}$, and its $^\bullet$OH formation potential is ~50 times higher. The extent of $^\bullet$OH generated increased with the concentration of the hydroxyphenol and chlorine, but the $^\bullet$OH yield (moles formed per mole of hydroxyphenol eliminated), decreased due to the formation of the quinone, that acts as $O_2^{\bullet-}$ scavenger. The yield was almost not affected by the pH ($6 \leq$ pH ≤ 7.5), whereas a strong impact of dissolved O_2 was observed. The $^\bullet$OH production was null in absence of O_2 and 2.5–3 times higher at oxygen saturated conditions compared to air-saturated. Contrary to chlorination, during bromination of hydroquinone $^\bullet$OH was not formed, which can be attributable to a much faster consumption of the oxidant, with no chance for $O_2^{\bullet-}$ to react with bromine.

Formation of $^\bullet$OH during the chlorination of different NOM extracts (SRHA, SRFA, PLFA and Nordic Lake NOM) and water from Lake Greifensee (Switzerland) was also studied using terephthalic acid as $^\bullet$OH scavenger. For SRHA, SRFA and Nordic Lake NOM (all of allochthonous origin and presenting high electron-donating capacity, EDC), $^\bullet$OH yields expressed as moles formed per mole of DOC_0 (%), were between 1.1 and 2.0, similar to that of hydroquinone (~1.5). For PLFA and Lake Greifensee water (autochthonous, lower EDC) much lower $^\bullet$OH yields were observed (0.1–0.3). Both chlorination rate and EDC, the later favouring the formation/stabilization of $O_2^{\bullet-}$, seem to be key factors involved in $^\bullet$OH generation during the chlorination of NOM. A mechanism for these findings is proposed based on kinetic simulations of hydroquinone chlorination at pH 7.

1. Introduction

Dissolved organic matter (DOM) is typically the main sink for oxidants commonly applied in drinking water treatment (Wenk et al., 2013; von Gunten, 2018). The oxidants react with electron-rich functional groups such as phenolic moieties, amines, olefines, etc., partially leading to the formation of low molecular weight organic disinfection byproducts (DBPs) (Lee et al., 2007; Bond et al., 2012; von Sonntag and von Gunten, 2012; Le Roux et al., 2016). Among the different structures present in DOM, phenolic moieties are highly reactive towards many different oxidants. The content of aromatic moieties in DOM has been usually measured in terms of the specific ultraviolet absorbance at 254 nm, $SUVA_{254}$ (Weishaar
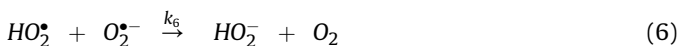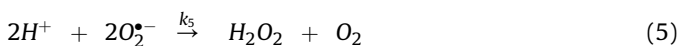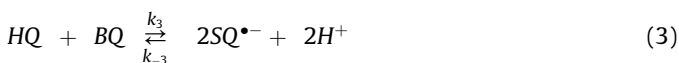
Nomenclature

BB	borate buffer
BQ	*p*-benzoquinone
BZ	benzene
CAT	catechol
•CHDt	cyclohexadienyl-type radical
•CHDHPt	cyclohexadienylhydroperoxide-type radical
DBPs	disinfection byproducts
DMSO	dimethyl sulfoxide
DNPH	2,4-dinitrophenylhydrazine
DOC	dissolved organic carbon
DOM	dissolved organic matter
DPD	diethyl-*p*-phenylene diamine
EDC	electron donating capacity
ET	electron transfer
FAB	free available bromine
FAC	free available chlorine
FAL	formaldehyde
GAL	gallic acid
HQ	hydroquinone
hTPA	2-hydroxyterephthalic acid
IC	inorganic carbon
IHSS	International Humic Substances Society
LG	Lake Greifensee
MeHQ	methylhydroquinone
NF$^-$	nitroform anion
NL-NOM	Nordic Lake natural organic matter
NOM	natural organic matter
•OHFP	total formation potential of •OH
•OHFP$_{air\ sat}$	total formation potential of •OH at air-saturated conditions
PBS	phosphate buffer
PHEN	phenol
PLFA	Pony Lake fulvic acid
RES	resorcinol
SQ•$^-$	semiquinone
SRFA	Suwannee River fulvic acid
SRHA	Suwannee River humic acid
SUVA$_{254}$	specific UV absorbance at 254 nm (L (mg DOC m)$^{-1}$)
TAN	tannic acid
TBA	*tert*-butyl alcohol
T$_{exp}$	experimental temperature
T$_{model}$	kinetic model temperature
TNM	tetranitromethane
TPA	terephthalic acid

et al., 2003), however, recently more specific measurements such as the electron-donating-capacity (EDC) are being used as a proxy of the phenolic content (Aeschbacher et al., 2012; Walpen et al., 2016; Önnby et al., 2018). Although, in general, phenolic structures react with chlorine by electrophilic aromatic substitution (EAS) forming chlorophenols, recent studies have demonstrated that chlorination of *ortho* and *para* hydroxyphenols occurs via an electron transfer (ET) with the formation of the corresponding quinones. These reactions are likely responsible for the high initial hypohalous acid consumption by DOM through ET reactions (Criquet et al., 2015).

The chemistry of *o*- and *p*-hydroxyphenols in water is complex. According to Eyer (1991), hydroquinone (HQ) can be oxidized by dissolved oxygen in aqueous solution through the following mechanism, based on the hydroquinone/semiquinone/benzoquinone (HQ/SQ•$^-$/BQ) equilibria:

$$HQ + O_2 \overset{K_1}{\rightleftharpoons} O_2^{\bullet-} + SQ^{\bullet-} + 2H^+ \tag{1}$$

$$SQ^{\bullet-} + O_2 \overset{k_2}{\underset{k_{-2}}{\rightleftharpoons}} BQ + O_2^{\bullet-} \tag{2}$$

$$HQ + BQ \overset{k_3}{\underset{k_{-3}}{\rightleftharpoons}} 2SQ^{\bullet-} + 2H^+ \tag{3}$$

$$HO_2^{\bullet} \overset{K_4}{\rightleftharpoons} O_2^{\bullet-} + H^+ \tag{4}$$

$$2H^+ + 2O_2^{\bullet-} \overset{k_5}{\rightarrow} H_2O_2 + O_2 \tag{5}$$

$$HO_2^{\bullet} + O_2^{\bullet-} \overset{k_6}{\rightarrow} HO_2^- + O_2 \tag{6}$$

At pH $\leq$ 7 equilibrium 1 is almost completely displaced to the left ($K_1 \sim 10^{-14}$ at pH 7, room temperature and air saturated, Eyer, 1991), and the oxidation of HQ to SQ•$^-$ by O_2, with generation of superoxide radical ($O_2^{\bullet-}$) is minimal. If SQ•$^-$ were formed, it would
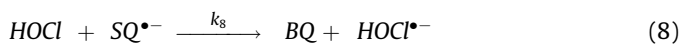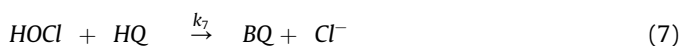
be quickly oxidized by O_2 to BQ (reaction 2, $k_2 = 5 \times 10^4$ M^{-1} s^{-1} at pH 7 and room temperature, Eyer, 1991), under formation of more $O_2^{\bullet-}$. BQ could then react with HQ ($k_3 = 58$ M^{-1} s^{-1}, $k_{-3} = 8 \times 10^7$ M^{-1}s^{-1} at pH 7, Yamazaki and Ohnishi, 1966), and also with $O_2^{\bullet-}$ ($k_{-2} = 10^9$ M^{-1} s^{-1} at pH 7, Eyer, 1991), both reactions leading to SQ•$^-$. With a $pKa = 4.8$ for equilibrium 4 (Bielski et al., 1985), at pH 7 the formation of hydroperoxyl radical (HO$_2^{\bullet}$) from superoxide protonation is expected to be very low, whereas $O_2^{\bullet-}$ disproportionation to H_2O_2 (reaction 5) is slow leading to a certain stability of $O_2^{\bullet-}$ in solution under these conditions (Sheng et al., 2014). Although the reaction between HO$_2^{\bullet}$ and $O_2^{\bullet-}$ to HO$_2^-$ has a high second-order rate constant ($k_6 = 9.7 \times 10^7$ M^{-1} s^{-1}, Sheng et al., 2014), at pH 7 this reaction is not favored due to the low concentration of HO$_2^{\bullet}$ (~0.6% of [$O_2^{\bullet-}$]).

In the above mechanism the possible reaction between HQ and $O_2^{\bullet-}$ was not considered. For this reaction, a second-order rate constant of 1.7×10^7 M^{-1} s^{-1} was reported by Rao and Hayon (1975), in disagreement with the findings of Nadezhdin and Dunford (1979), among others, who determined a second-order rate constant of 1.7×10^4 M^{-1}s^{-1} for the HQ/HO$_2^{\bullet}$ reaction. Since HO$_2^{\bullet}$ is a stronger oxidant than $O_2^{\bullet-}$, the rate constant of HQ-$O_2^{\bullet-}$ reaction is expected to be $< 1.7 \times 10^4$ M^{-1} s^{-1}.

According to the mechanism provided in reactions 1–6, superoxide radical will not be formed in absence of dissolved O_2 and its steady state concentration will be very low in an aerated medium at pH $\leq$ 7.

The presence of an agent that can oxidize HQ to BQ could promote the formation of SQ•$^-$ through reaction 3 and hence the generation of $O_2^{\bullet-}$ (reaction 2). As stated before, Criquet et al. (2015) determined that chlorine and bromine react with *o*- and *p*-hydroxyphenols, HQ among them, via ET, with formation of the corresponding quinones. In the case of HQ, the apparent second-order rate constant of its reaction with free available chlorine (FAC, sum of [HOCl] and [ClO$^-$]) at pH 7 (reaction 7; $k_7 = 21.6$ M^{-1} s^{-1} measured in terms of BQ formation) is comparable to that of reaction 3. Hence, depending on the experimental conditions as BQ is formed, some SQ•$^-$ can be generated (reaction 3), thereby promoting the formation of $O_2^{\bullet-}$. Also, the oxidation of

$SQ^{\bullet-}$ by HOCl, with formation of $HOCl^{\bullet-}$ (reaction 8), cannot be ruled out.

$$HOCl \; + \; HQ \quad \overset{k_7}{\rightarrow} \quad BQ + \; Cl^- \tag{7}$$

$$HOCl \; + \; SQ^{\bullet-} \quad \xrightarrow{\;\; k_8 \;\;} \quad BQ + \; HOCl^{\bullet-} \tag{8}$$

According to Candeias et al. (1993), superoxide reacts with HOCl to form $^\bullet OH$ (reaction 9; $k_9 = 7.5 \times 10^6$ M^{-1} s^{-1}, determined by monitoring the decay of $O_2^{\bullet-}$; Long and Bielski, 1980).

$$HOCl \; + \; O_2^{\bullet-} \quad \overset{k_9}{\rightarrow} \quad {}^\bullet OH \; + \; Cl^- \; + \; O_2 \tag{9}$$
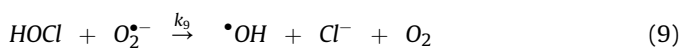
Therefore, if during HQ chlorination $SQ^{\bullet-}$ (and hence, $O_2^{\bullet-}$) is generated, hydroxyl radicals could be formed through reaction 9. Also, if reaction 8 develops, $HOCl^{\bullet-}$ would lead to $^\bullet OH$ formation through reaction 10 ($k_{10} = 6.1 \times 10^9$ s^{-1} and $k_{-10} = 4.3 \times 10^9$ M^{-1} s^{-1}, Jayson et al., 1973).

$$HOCl^{\bullet-} \quad \overset{k_{10}}{\underset{k_{-10}}{\rightleftarrows}} \quad {}^\bullet OH \; + \; Cl^- \tag{10}$$

A previous study revealed that an initial bromination of natural organic matter (NOM) mainly occurs through ET instead of EAS (Criquet et al., 2015). Hence, with the presence of phenols being structural moieties of NOM and in analogy to bromination, formation of $SQ^{\bullet-}$ during chlorination of NOM, with a concomitant formation of $HOCl^{\bullet-}$ and/or $O_2^{\bullet-}$ and subsequently $^\bullet OH$, cannot be ruled out.

Because of the short lifetime of hydroxyl radicals, it is common to use scavengers to determine their formation (Flyunt et al., 2003; Rodríguez et al., 2015). Moreover, if the product from the reaction between $^\bullet OH$ and a scavenger is known and can be measured, the extent of the formation of $^\bullet OH$ can be estimated. In addition, it is also important to exclude reactions of the scavenger and/or the reaction products with other substances present in the reaction medium (reagents and/or intermediates and/or products). Therefore, the following criteria need to be considered for the selection of a scavenger to quantify $^\bullet OH$ formation: (i) The reactivity of the scavenger, the organic surrogate (hydroxyphenols or NOM in this case) and the oxidant (chlorine in this study) towards the radical species; (ii) the nature of the products formed from the reaction between the scavenger and the radical (stability, reactivity towards oxidants, etc.); (iii) easy detection and quantification of the products; and (iv) the reactivity of the scavenger, the transformation products and the organic surrogate towards the oxidant. Furthermore, the scavenger has to be present in a sufficiently high concentration, so that a fraction of >95% of the $^\bullet OH$ is scavenged. Even though the product from the reaction between the scavenger and $^\bullet OH$ is an indicator of the generation of this species, there are some uncertainties on its quantification due to possible effects of the reaction conditions on the product yield (moles of product formed per mole of $^\bullet OH$ generated).

In this study, to investigate the formation of $^\bullet OH$, dimethyl sulfoxide (DMSO), tert-butyl alcohol (TBA), benzene (BZ) and terephthalic acid (TPA) were initially selected as scavengers. However, DMSO, that reacts with $^\bullet OH$ to form methane sulfinic acid (MSI) ($k_{^\bullet OH\text{-}DMSO} = 4.5 \times 10^9$ M^{-1} s^{-1}; Bardouki et al., 2002), also has a relatively high reactivity with FAC ($k_{FAC\text{-}DMSO} = 315$ M^{-1} s^{-1} at pH 7, 20 °C; Amels et al., 1997), wherefore its use is impossible for this system. The second order rate constants for the reactions of the different $^\bullet OH$ scavengers towards $^\bullet OH$ and FAC (pH 7 and 25 °C) and their reaction products are provided in Table 1.

The main products from the reaction between $^\bullet OH$ and TBA ($k_{^\bullet OH\text{-}TBA} = 6 \times 10^8$ M^{-1} s^{-1}; Buxton et al., 1988) in presence of oxygen are formaldehyde (FAL; ~25% of $^\bullet OH$; Flyunt et al., 2003), acetone, 2-hydroxy-2-methylpropanal and 2-methyl-2-hydroxypropanol, as well as considerable amounts of $HO_2^\bullet/O_2^{\bullet-}$ (Schuchmann and von Sonntag, 1979; Cederbaum et al., 1983; Flyunt et al., 2003). Neither TBA nor FAL reacts with HOCl. The reactivity/stability of other reaction products is unknown.

In aqueous solution and in presence of dissolved oxygen the reaction between $^\bullet OH$ (generated radiolytically) and BZ ($k_{^\bullet OH\text{-}BZ} = 7.8 \times 10^9$ M^{-1} s^{-1}; Buxton et al., 1988) proceeds through the formation of a hydroxycyclohexadienyl radical that further reacts with O_2, to mainly phenol (Pan et al., 1993). The molar phenol yields were found in the range of 53–93% depending on the pH, and $O_2^{\bullet-}$/$HO_2^\bullet$, small amounts of various aldehydes and formic acid were also formed. By photolysis of aerated NO_3^- to produce $^\bullet OH$ at pH ~ 6, the molar phenol yield was 95% (Deister et al., 1990). An average value of 85% has been adopted by different authors (Dong and Rosario-Ortiz, 2012). Contrary to BZ, which does not react with FAC, phenol (PHEN) reacts with an apparent second order rate constant $k_{FAC\text{-}PHEN} = 18$ M^{-1} s^{-1}, at pH 7 and 25 °C (Gallard and von Gunten, 2002).

The reaction of $^\bullet OH$ with TPA in aqueous solution ($k_{^\bullet OH\text{-}TPA} = (3.3–4.4) \times 10^9$, Fang et al., 1996; Page et al., 2010; Charbouillot et al., 2011) results in the formation of the corresponding cyclohexadienyl-type radical intermediate with a yield of about 85%. In presence of dissolved oxygen as the only oxidant, this radical intermediate reacts with O_2 generating 2-hydroxyterephthalic acid (hTPA) and $O_2^{\bullet-}/HO_2^\bullet$ (Fang et al., 1996). The molar yield of hTPA based on moles of $^\bullet OH$ produced is ~30% at pH 7 and 25 °C and slightly increasing with increasing pH and temperature (Charbouillot et al., 2011). The reactivity of the cyclohexadienyl-type radical formed from the TPA-$^\bullet OH$ reaction with O_2 is ~30 times lower than that of the radical formed from BZ-$^\bullet OH$ reaction (Fang et al., 1995). Because of that, in presence of a stronger oxidant such as $IrCl_6^{2-}$, the hTPA yield can increase to up to 85% without formation of $O_2^{\bullet-}/HO_2^\bullet$ (Fang et al., 1996). Since there are no data in literature about the reactivity of TPA nor hTPA towards FAC, the corresponding apparent second-order rate constants (pH 7 and 25 °C) have been experimentally determined in this study.

The above mechanism (reactions 1–10) suggests that $^\bullet OH$ might be formed during the chlorination of hydroxy-phenolic compounds. However, so far, there is no experimental evidence for this process. The main objective of this study was to determine whether chlorination of NOM leads to $^\bullet OH$ formation and identify the main NOM structures involved. To this end, different o-, m- and p-hydroxyphenols (hydroquinone, catechol, resorcinol, gallic and tannic acid) and NOM extracts (humic and fulvic acids) were chlorinated, and the formation of $^\bullet OH$ and the role of $O_2^{\bullet-}$ were investigated with the aid of multiple radical scavengers. The influences of hydroxyphenol, NOM, FAC and dissolved oxygen concentrations as well as pH on $^\bullet OH$ production were also studied. From the results obtained a kinetic model for $^\bullet OH$ formation during hydroquinone chlorination at pH 7 was developed to support the proposed mechanism.

2. Materials and methods

2.1. Chemicals

With the exception of the sodium hypochlorite solution (10−15% active chlorine, Sigma-Aldrich, reagent grade), all organic and inorganic compounds (purchased from Sigma-Aldrich, Fluka Analytical, Merck or Carlo Erba), were of analytical grade or higher and used without further purification. Stock solutions of the

Table 1
Second order rate constants for the reactions of different scavengers with hydroxyl radical (•OH) and HOCl and the corresponding reaction products.

Scavenger	Second order rate constant for the reaction with •OH $k_{•OH}$, $M^{-1}s^{-1}$	Selected product from the reaction with •OH	Second order rate constant for the reaction with FAC k_{FAC}, $M^{-1}s^{-1}$	Second order rate constant for the reaction of the product with FAC, $k*_{FAC}$, $M^{-1}s^{-1}$
Dimethyl sulfoxide (DMSO)	4.5×10^9 (Bardouki et al., 2002)	Methanesulfinic acid (MSI)[a]	$k_{FAC-DMSO} = 315$, pH 7, 20 °C (Amels et al., 1997)	?
tert-butyl alcohol (TBA)	6×10^8 (Buxton et al., 1988)	Formaldehyde (FAL) [b]	NR	NR
Benzene (BZ)	7.8×10^9 (Buxton et al., 1988)	Phenol (PHEN) [a]	NR	$k_{FAC-PHEN} = 18$, pH 7, 25 °C (Gallard and von Gunten, 2002)
Terephthalic acid (TPA)	3.3×10^9 (Fang et al., 1996)	2-hydroxy-TPA (hTPA) [a]	$k_{FAC-TPA} < 0.003$, pH 7, 25 °C (this study)	$k_{FAC-hTPA} = 0.147$, pH 7, 25 °C (this study)

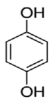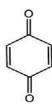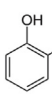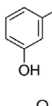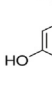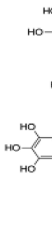FAC: Free available chlorine = [HOCl] + [ClO⁻].
[a] Is the main product.
[b] Is not the main product; NR: No Reaction.

selected hydroxyphenols (15 mM for hydroquinone (HQ), catechol (CAT), resorcinol (RES) and gallic acid (GAL); 2.5 mM for tannic acid (TAN)), were freshly prepared in Milli-Q ultrapurified water. Their structures are presented in Table 2 together with the corresponding second order rate constants for the reactions with FAC, •OH and $O_2^{•-}$.

The NOM extracts were purchased from the International Humic Substances Society (IHSS) and used as received: Suwannee River humic acid II (SRHA, catalogue number: 2S101H), Suwannee River fulvic acid II (SRFA, catalogue number: 2S101F) and Nordic Lake NOM (NL-NOM, catalogue number: 1R108N), representing organic materials from allochthonous origin; and Pony Lake fulvic acid (PLFA, catalogue number: 1R109F), as a representative of autochthonous NOM in aquatic systems. Some of their characteristics are summarised in Table S1 (supplementary information, SI). A given amount of each extract was dissolved in pH 7 phosphate buffer (PBS, 1 mM) to obtain stock solutions of 20 mg L⁻¹. Chlorination of a filtered (0.45 μm nylon membrane, VWR) water from Lake Greifensee (LG) (Canton of Zurich, Switzerland), was also carried out. The main characteristics of LG water were: DOC 3.3 mg L⁻¹, alkalinity 355 mg L⁻¹ $CaCO_3$, and pH 8.37. Stock NOM solutions and LG water were stored at 4 °C until used.

Table 2
Structures of the selected hydroxy-phenols and the apparent second order rate constants for their reactions with FAC, •OH and $O_2^{•-}$ at pH 7.

Compound	Structure	k_{FAC} (pH 7, 25 °C), $M^{-1}s^{-1}$	$k_{•OH}$, $M^{-1}s^{-1}$	$k_{O2•-}$, $M^{-1}s^{-1}$
Hydroquinone (HQ) $C_6H_6O_2$; MW 110.11		21.6 (Criquet et al., 2015)	1.2×10^{10} (Gurol and Vatistas, 1987)	$<1.7 \times 10^4$ (Nadezhdin and Dunford, 1979)
p-benzoquinone (BQ) $C_6H_4O_2$; MW 108.09		~3 (This study)	6.6×10^9 (Schuchmann et al., 1998)	10^9 (Eyer, 1991)
Catechol (CAT) $C_6H_6O_2$; MW 110.11		217.5 (Criquet et al., 2015)	1.1×10^{10} (Buxton et al., 1988)	2.7×10^5 (Bielski et al., 1985)
Resorcinol (RES) $C_6H_6O_2$; MW 110.11		~4000 (Rebenne et al., 1996)	1.2×10^{10} (Buxton et al., 1988)	2 (Bielski et al., 1985)
Gallic acid (GAL) $C_7H_6O_5$; MW 170.12		1600 (Criquet et al., 2015)	10^{10} (Dwibedy et al., 1999)	2.3×10^3 (Huisman et al., 2004)
Tannic acid (TAN) $C_{76}H_{52}O_{46}$; MW 1701.2		1.9×10^4 (Criquet et al., 2015)	3×10^{10} (Bors and Michel, 1999)	

A FAC stock solution (~50 mM) was prepared every week by dilution of a commercial hypochlorite solution with ultrapurified water and stored at 4 °C. HOBr was obtained from the reaction between 1 mM Br$^-$ and 1.1 mM ozone at pH 4 (5 mM PBS) during 30 min, purging any residual ozone with nitrogen for 1−2 h (Heeb et al., 2017). The lower reaction time applied compared to that of Heeb et al., (2017) is probably the reason why the final HOBr concentration was lower than expected (~0.7 mM instead of ~1 mM).

Stock solutions of the different scavengers were prepared in ultrapurified water: tert-butyl alcohol (TBA) 3.5 M; saturated aqueous benzene (BZ) ~ 23 mM, stirred overnight and kept in a fume hood; terephthalic acid (TPA) 50 mM, adjusted to pH 6.5 by adding some drops of concentrated NaOH; and MnCl$_2$·4H$_2$O 20 mM, the latter used as a superoxide scavenger. When tetranitromethane (TNM) was used as superoxide scavenger, 4 μL of TNM 8.2 M (pure compound) was added to 20 mL of the reaction medium (final [TNM] = 1.65 mM) in the fume hood.

2.2. Analytical methods

Stock solutions of chlorine and bromine were photometrically standardized at pH 11 before use (ϵ_{ClO-} at 292 nm = 350 M^{-1} cm^{-1}, Hand and Margerum, 1983; ϵ_{BrO-} at 330 nm = 327 M^{-1} cm^{-1}, Heeb

et al., 2017). Residual concentrations of FAC were determined using a colorimetric method based on diethyl-p-phenylene diamine (DPD), measuring the absorbance at 515 nm (Rodier et al., 2009).

The selected hydroxyphenols (HQ, CAT, RES, GAL and TAN), p-benzoquinone (BQ), formaldehyde (FAL), phenol (PHEN), and 2-hydroxyterephthalic acid (hTPA), were measured by a high-performance liquid chromatography system (HPLC Dionex Ultimate 3000) equipped with a Nucleosil 100-5 C18 column (125 × 3 mm, 5 μm, 100 A, Macherey-Nagel) with UV diode array and fluorescence detectors. The column temperature and flow were set as 30 °C and 0.8 mL min^{-1}, respectively, using 0.1% H$_3$PO$_4$ in ultrapurified water (A) and methanol (B) to prepare the mobile phases. In all cases, 100 μL samples were injected except for hTPA (20 μL).

Formaldehyde (FAL) was firstly derivatized with 2,4-dinitrophenylhydrazine (DNPH), to form the corresponding hydrazone, and then analysed by HPLC-DAD at 360 nm (U.S. EPA, 1996). Acetone and BQ, if present, were also quantified by this method.

A description of the preparation of reagents, conditions of the HPLC analyses, measuring ranges and limits of detection (LOD) and quantification (LOQ) are provided in **Text S1 (SI)**.

The nitroform anion (NF$^-$) formed from the tetranitromethane (TNM) reduction by O$_2^{\bullet-}$ was determined spectrophotometrically at 350 nm (ϵ_{350nm} = 14600 M^{-1}cm^{-1}; Rabani et al., 1965).

The dissolved organic carbon (DOC) and inorganic carbon (IC) content in LG water were measured using a Shimadzu total organic carbon (TOC) analyzer. Initial DOC concentration (DOC$_0$) of the hydroxyphenols and NOM extract solutions was calculated from their molecular structures and chemical composition, respectively.

2.3. Experimental procedures

2.3.1. Chlorination of phenolic surrogates, NOM extracts and LG water in the presence of •OH scavengers

To determine the formation of •OH during chlorination, 0.4 mL phosphate buffer (PBS) 0.5 M (pH 6−7.5), and fixed volumes of hydroxyphenol solutions (or NOM solutions), radical scavenger stock solutions and ultrapurified water were added, to obtain the desired concentrations in a final volume of 20 mL (22 mL amber glass vials). In the case of LG water, only the scavenger solution was added, decreasing the pH from 8.37 to 7.85.

After mixing, different volumes of a FAC stock solution were added to each vial while stirring and the vials were closed. A control sample was always prepared under the same conditions but without adding FAC. The mixtures were allowed to react at room temperature for 1−72 h (depending on the nature of the surrogate and the concentration of reactants) and then analysed by HPLC. In some cases bromine instead of chlorine was added.

To establish the initial concentrations of all reagents, the reactivity of the •OH scavenger, the organic surrogates and FAC towards •OH was taken into account to ensure that more than 95% of the generated •OH (f(•OH)≥0.95), is captured by the •OH scavenger, according to the following equation:

$$f(^{\bullet}OH) = \frac{k_{^{\bullet}OH-scavenger}[^{\bullet}OH\ scavenger]}{k_{^{\bullet}OH-scavenger}[^{\bullet}OH\ scavenger] + k_{^{\bullet}OH-hydroxyphenol}[hydroxyphenol] + k_{^{\bullet}OH-HOCl}[HOCl] + k_{^{\bullet}OH-ClO^-}[ClO^-]} \quad (11)$$

where $k_{^{\bullet}OH-scavenger}$ represents the second order rate constant for the reaction between •OH and the selected scavenger (Table 1); $k_{^{\bullet}OH-hydroxyphenol}$ the second order rate constant for the reaction between •OH and the phenolic surrogate (Table 2); $k_{\bullet OH-HOCl}$ (1.21 × 10^9 M^{-1}s^{-1}, Bulman et al., 2019) and $k_{\bullet OH-ClO-}$ (6.37 × 10^9 M^{-1} s^{-1}; Bulman et al., 2019), are the second order rate constants for the reactions of •OH with HOCl and ClO$^-$, respectively. The [•OH scavenger], [hydroxyphenol], [HOCl] and [ClO$^-$] are the initial molar concentrations of each reactant, the last two determined taking into account the pH of the medium, equilibrium 12, and the concentration of FAC ([FAC] = [HOCl] + [ClO$^-$]). Since the second order rate constants for the reactions between •OH and H$_2$PO$_4^-$/HPO$_4^{2-}$ are extremely low (2 × 10^4 and 1.5 × 10^5 M^{-1} s^{-1}, respectively; Buxton et al., 1988), at the tested conditions (PBS 10 mM) they can be neglected as •OH scavengers.

$$HOCl \underset{}{\overset{pKa=7.49}{\rightleftharpoons}} ClO^- + H^+ \quad (12)$$
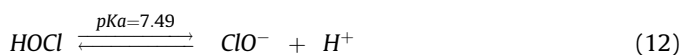
Thus, for [hydroxyphenol]$_0$ ≤ 62.5 μM, molar [FAC]$_0$/[hydroxyphenol]$_0$ ratios ≤ 2.5 and pH ≤ 7.5, 50 mM TBA, 10 mM BZ and 4 mM TPA were used to fulfill a >95% scavenging criteria for f(•OH) according to equation (11) (see Table S2 in SI for calculated values).

To investigate the participation of O$_2^{\bullet-}$, a similar procedure was applied by adding different amounts of a 15 mM BQ stock solution, pure TNM or 20 mM Mn(II) (as MnCl$_2$·4H$_2$O), in the latter case filtering the samples (0.45 μm nylon filter) before the HPLC analysis.

When needed, the dissolved O$_2$ concentration in the reaction medium was increased or reduced by purging with pure O$_2$ or N$_2$, respectively. When BZ was used, bubbling was performed before adding the scavenger to avoid losses by stripping.

2.3.2. Determination of chlorine demand (72 h) of NOM extracts and LG water

In a series of 22 mL amber glass vials, 0.4 mL of 0.5 M PBS pH 7 and a fixed volume of NOM extract stock solutions were added, thereafter diluted to 20 mL with ultrapurified water. After mixing, to obtain different $[FAC]_0/[DOC]_0$ molar ratios a predetermined volume of a FAC stock solution was added to each vial while stirring and the vials were closed. The mixtures were allowed to react at room temperature in the dark, and after 72 h the residual FAC was analysed. For LG water, the procedure was the same but without adding PBS or ultrapurified water. Once the chlorine demand (μM) of each NOM solution was determined, the specific chlorine demand was calculated by dividing this value by the DOC_0 (μM) content.

2.3.3. Determination of the apparent second order rate constants for the reactions between chlorine and TPA, hTPA or BQ at pH 7 (10 mM PBS) and 25 °C

Apparent second order rate constants for the reactions of TPA, hTPA or BQ with chlorine at pH 7 (10 mM PBS, 25 °C), were determined in excess of FAC (pseudo-first order conditions; see experimental conditions in Fig. S1, SI), by measuring the evolution of the parent compounds (TPA and hTPA by HPLC-DAD/fluorescence; BQ by the decrease of the absorbance at 247 nm). In all cases but BQ, residual chlorine was quenched before the analysis by adding a few μL of a concentrated solution of $Na_2S_2O_3$ (0.5 M). For TPA, experiments in excess of TPA (4 mM) were also performed measuring the evolution of residual FAC ($[FAC]_0 = 45$ μM). For BQ, a competition kinetics method was also applied using phenol as competitor ($k_{FAC-PHEN} = 18$ M^{-1} s^{-1} at pH 7, 25 °C; Gallard and von Gunten, 2002). In this case, vials containing BQ (50 μM) and PHEN (5−10 μM) (10 mM PBS, pH 7 at 25 °C), were dosed with different volumes of a FAC stock solution to obtain $[FAC]_0$ in the range of 0−50 μM. The samples were mixed, and after a reaction time of 3 h, the final concentrations of BQ and PHEN were determined by HPLC. In all cases, control samples were prepared in absence of chlorine. All the experiments were carried out at least in duplicate.

2.3.4. Modelling of •OH generation during chlorination of HQ

The kinetics of the formation of •OH during HQ chlorination at pH 7, 25 °C and air saturated conditions (concentration of dissolved oxygen assumed to be 3×10^{-4} M), was modeled by the Tenua kinetic simulator (http://bililite.com/tenua/).

3. Results and discussion

3.1. Determination of •OH formation from hydroquinone chlorination

3.1.1. Influence of the nature of the selected •OH scavengers on HQ chlorination

In a first series of experiments, chlorination of an air-saturated HQ solution 62.5 μM (DOC 4.5 mg L^{-1}) at pH 7 (PBS 10 mM) and room temperature (22 ± 2 °C) was carried out, using different molar $[FAC]_0/[HQ]_0$ ratios, in absence/presence of the selected •OH scavengers: TBA 50 mM, BZ 10 mM or TPA 4 mM (Fig. 1).

Under these experimental conditions, and as expected due to their low reactivity towards FAC (see Table 1 and Fig. S1, SI) the scavengers had practically no effect on the extent of HQ oxidation. Thus, for a given $[FAC]_0/[HQ]_0$ ratio, the extent of HQ abatement after 1.5 h contact time (Fig. 1a) was very similar regardless of the presence of a scavenger. Furthermore, the HQ abatement (solid symbols) corresponded well with the BQ formed (open symbols), i.e., the BQ yields were close to 1 mole per mole of HQ oxidized. For

$[FAC]_0/[HQ]_0$ ratios > 1.5, a decrease in the final BQ concentration is observed, most probably due to its reaction with FAC ($k_{FAC-BQ} = 3$ M^{-1} s^{-1} at pH 7, 25 °C obtained in this study; Fig. S1, SI). Also, as the dose of FAC increased, the BQ concentration was higher in presence of a scavenger, which could indicate that under these conditions some BQ abatement is prevented. The apparent global stoichiometry of the chlorine-HQ reaction was close to 2 mol of chlorine per mole of HQ consumed (Fig. 1b), which is consistent with previous observations (Criquet et al., 2015).

#### 3.1.2. Influence of the nature of the scavenger on •OH quantification

In Fig. 2a, the concentrations of FAL (from TBA), PHEN (from BZ) or hTPA (from TPA) formed from chlorination (1.5 h contact time) of air-saturated HQ 62.5 μM solution (pH 7), for different $[FAC]_0/[HQ]_0$ molar ratios are shown. In absence of FAC (control), FAL, PHEN or hTPA were not detected. The FAL concentration was much lower than PHEN or hTPA, results that cannot be attributable to the low FAL yield of the TBA-•OH reaction (~25%; Flyunt et al., 2003). Moreover, the FAL concentration initially increased with increasing molar $[FAC]_0/[HQ]_0$ ratios and decreased for ratios > 0.5. These results indicate that, for the tested conditions, FAL and acetone (not shown) are not stable in solution due to unknown secondary reactions. Therefore, in the further experiments the formation of FAL from TBA was not considered to determine the formation of •OH from HQ chlorination.

For molar $[FAC]_0/[HQ]_0$ ratios $\leq$ 0.5, the PHEN and hTPA concentrations were similar despite the different yields of PHEN (from BZ + •OH) and hTPA (from TPA + •OH) reported in air saturated and neutral pH conditions (~85% and 30%, respectively). As it will be discussed in the kinetics section, this could indicate that in presence of chlorine, similarly to what was observed in presence of $IrCl_6^{2-}$ (Fang et al., 1996), the yield of hTPA is higher than when using O_2 as the only oxidant. For $[FAC]_0/[HQ]_0 > 1$ the extent of PHEN formation was clearly lower than for hTPA and it was negligible for $[FAC]_0/[HQ]_0 > 2$. Undoubtedly, these results are related to the reactivity of PHEN towards HOCl, which is about 100 times higher than for hTPA ($k_{FAC-hTPA} \sim 0.15$ M^{-1} s^{-1} at pH 7 and 25 °C; Table 2 and Fig. S1, SI).

The yield of PHEN or hTPA as moles formed per mole of HQ eliminated (%), is shown in Fig. 2b. For the lowest molar $[FAC]_0/[HQ]_0$ ratio, yields of PHEN and hTPA were ~20% and ~15%, respectively. As the $[FAC]_0/[HQ]_0$ ratios increased, both yields decreased, in case of PHEN to < 5% for molar ratios $\geq$ 1.5, potentially due to the reaction of PHEN with chlorine. For hTPA, as will be discussed later, the decrease in the yield is probably related to a superoxide scavenging effect of the formed BQ, and remained almost constant at about 9% for molar $[FAC]_0/[HQ]_0$ ratios $\geq$ 0.5.

For the conditions tested, the compliance with equation (11) ($f(^\bullet OH) \geq 0.95$) was also experimentally corroborated as shown in Fig. S2 (SI) as an example, where the influence of the TPA concentration on hTPA formation from HQ chlorination ($[HQ]_0$ 62.5 μM; $[FAC]_0$ 93.7 μM), at pH 7 and room temperature, is presented. As observed, a constant hTPA concentration was determined when TPA >3 mM was added.

The fact that both PHEN and hTPA are detected implies that under the applied experimental conditions, chlorination of HQ leads to the formation of •OH. Moreover, to suppress the •OH -TPA reaction, the formation of hTPA was also tested in presence of high TBA concentrations. The results (Fig. S3, SI) indicate that TBA drastically inhibited the formation of hTPA. Therefore, it is very likely that •OH is the main species involved in hTPA formation and the same can be assumed for PHEN when BZ was used as a scavenger.
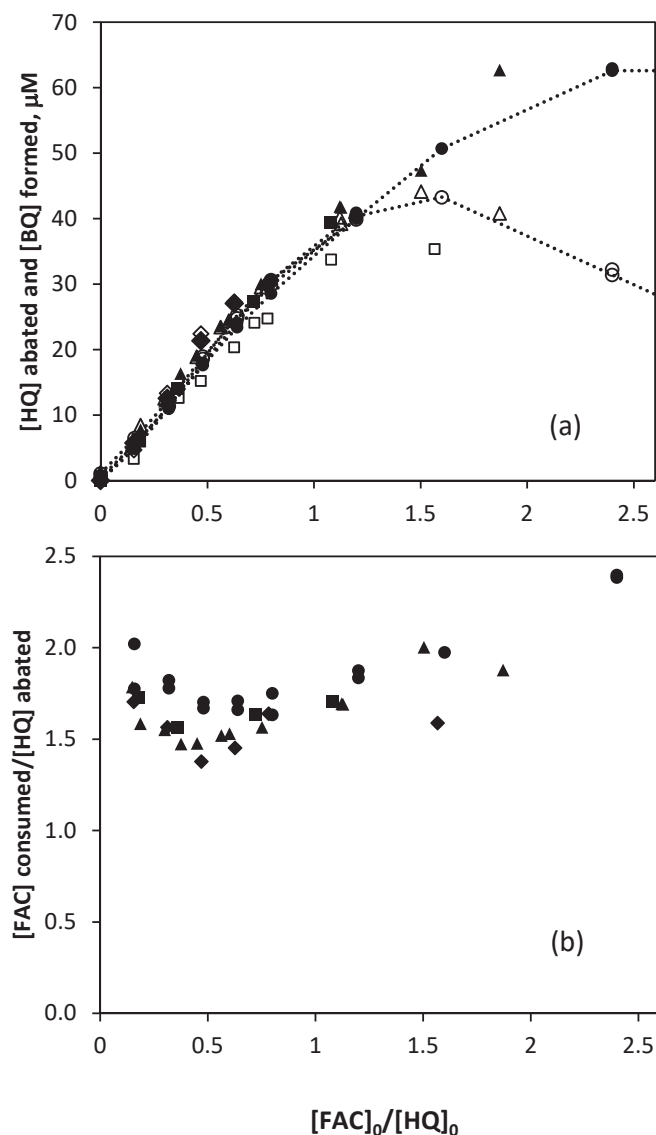
Fig. 1. (a) Influence of the different scavengers on the abatement of hydroquinone (HQ; solid symbols) and formation of benzoquinone (BQ; open symbols) as a function of the molar $[FAC]_0/[HQ]_0$ ratios; (b) FAC consumed per mole of HQ eliminated as a function of the molar $[FAC]_0/[HQ]_0$ ratios. ▲,△: 10 mM benzene (BZ); ●,O: 4 mM terephthalic acid (TPA); ◆,◇: 50 mM *tert*-butyl alcohol (TBA); ■, □: no scavenger. Experimental conditions: $[HQ]_0 = 62.5$ μM; air saturated PBS (10 mM), pH 7; $T_{exp} = 22 \pm 2$ °C; reaction time = 1.5 h. The lines in Fig. 1a are shown to guide the eye.

3.1.3. Influence of the initial concentration of HQ

The influence of the initial HQ concentration on •OH formation at pH 7 for TPA as •OH scavenger is shown in Fig. 3. As presented in Fig. 3a, for $[HQ]_0 < 15$ μM, the concentration of hTPA increased almost linearly as $[FAC]_0/[HQ]_0$ increased, whereas for higher $[HQ]_0$ a linearity can only be observed for low $[FAC]_0/[HQ]_0$ ratios, with hTPA concentrations approaching a plateau for higher values. The molar hTPA yields, based on moles of HQ abated (Fig. 3b), decrease with increasing $[HQ]_0$, approaching constant values at higher molar $[FAC]_0/[HQ]_0$ ratios. Similar results have been obtained for the PHEN yields when BZ was used as scavenger (Fig. S4, SI).

These observations could be at least partly explained by the nature of the intermediates and/or products formed during HQ chlorination. BQ, which reacts very fast with $O_2^{\bullet-}$ ($k_{-2} = 10^9$ M^{-1}s^{-1}), could compete with HOCl ($k_9 = 7.5 \times 10^6$ M^{-1} s^{-1}) for $O_2^{\bullet-}$, thereby
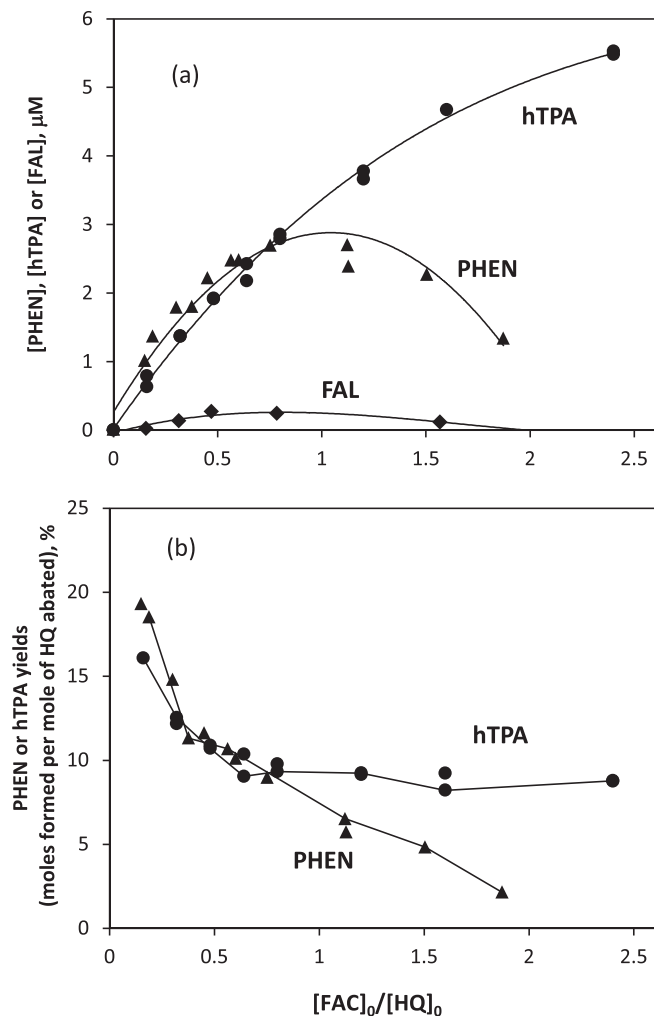
Fig. 2. Chlorination of HQ: Influence of the molar $[FAC]_0/[HQ]_0$ ratios on (a) phenol (PHEN) (▲), hydroxy-terephtalic acid (hTPA) (●) and formaldehyde (FAL) (◆) formation. (b) PHEN and hTPA yields from BZ and TPA, respectively. Experimental conditions: $[HQ]_0 = 62.5$ μM; TBA = 50 mM; BZ = 10 mM; TPA = 4 mM; air saturated PBS (10 mM), pH 7; $T_{exp} = 22 \pm 2°$; reaction time = 1.5 h. The lines are shown to guide the eye.

lowering the •OH yield. To test this, BQ (0−60 μM) was added to samples containing 62.5 μM HQ and 10 mM BZ. Under these conditions, BQ did not impact the $f(•OH)$ of the scavenger (Table S2, SI). The mixtures were chlorinated and PHEN was measured. Fig. 4 shows the evolution of the PHEN yields as a function of $[FAC]_0/[HQ]_0$ for experiments performed with/without initial BQ (see also Fig. S5, SI). For low molar $[FAC]_0/[HQ]_0$ ratios (and therefore low BQ formation from HQ chlorination), the addition of BQ clearly reduced the PHEN yield. For increasing molar $[FAC]_0/[HQ]_0$ ratios, this effect was compensated by the BQ formed from HQ oxidation. Hence, it can be hypothesized that BQ can become a superoxide scavenger (reaction −2), lowering the •OH yield.

In absence of FAC (control samples) the concentration of HQ varied very slightly during the reaction time considered (between 1.5 and 4 h), indicating that a contribution of reaction 1 (HQ autooxidation) to $O_2^{\bullet-}$ and $SQ^{\bullet-}$ formation was likely negligible. This means that BQ is mainly formed from HQ chlorination (reaction 7), allowing the formation of $SQ^{\bullet-}$ through reaction 3. Depending on the experimental conditions, the $SQ^{\bullet-}$ formed could be further oxidized to BQ by O_2 (reaction 2), with concomitant generation of $O_2^{\bullet-}$, and/or HOCl (reaction 8) to HOCl$^{\bullet-}$, which could also
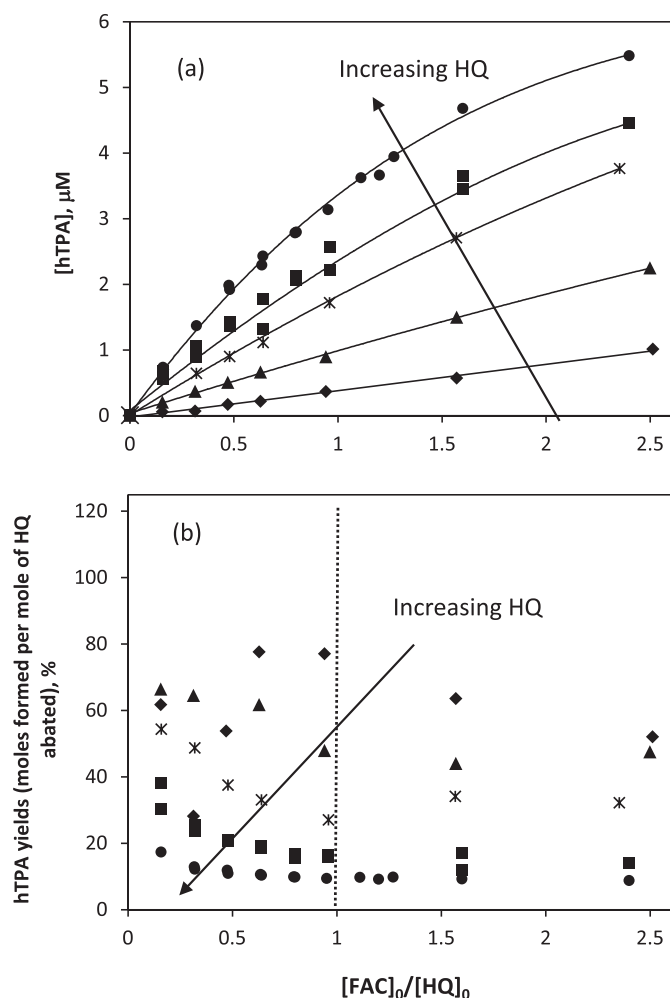
Fig. 3. Chlorination of HQ as a function of the molar $[FAC]_0/[HQ]_0$ ratio. Influence of the initial HQ concentrations on (a) hTPA formation and (b) hTPA yields. Symbols: ◆: $[HQ]_0 = 3.9$ μM; ▲: $[HQ]_0 = 7.8$ μM; ✳: $[HQ]_0 = 15.6$ μM; ■: $[HQ]_0 = 31.2$ μM; ●: $[HQ]_0 = 62.5$ μM. Experimental conditions: TPA = 4 mM; air saturated PBS (10 mM), pH 7; $T_{exp} = 22 \pm 2$ °C; reaction time = 1.5–4 h. The lines in Fig. 3a are shown to guide the eye.

contribute to •OH generation through reaction 10.

To test the potential role of superoxide radicals, experiments were performed with TNM or Mn(II) as $O_2^{\bullet-}$ scavengers. Unfortunately, due to the reactivity of TNM and Mn(II) towards HQ, that at the conditions tested was oxidized to BQ by these reagents in absence of chlorine, their use as $O_2^{\bullet-}$ scavenger seems to be impossible for this system (for further information see **Text S2,** SI).

3.1.4. Influence of pH

To test the influence of speciation of chlorine on •OH production from HQ chlorination, experiments were performed in the pH range 6–7.5 (PBS 10 mM, $[HQ]_0$ 62.5 μM, air saturated), using TPA as •OH scavenger. At pH > 7.5, HQ is not stable in solution due to its fast oxidation by O_2 (James et al., 1938; WHO, 1994; Criquet et al., 2015). At pH 7.5, the formation of a BQ ~1.5 μM was determined in the control sample (absence of chlorine), attributable to partial HQ autooxidation by O_2 through reactions 1–2.

Fig. 5 depicts hTPA concentrations and yields at different pH values for different molar $[FAC]_0/[HQ]_0$ ratios. A slight increase in the extent of hTPA formation with increasing pH is observed for higher $[FAC]_0/[HQ]_0$ ratios (Fig. 5a). However, since the extent of HQ
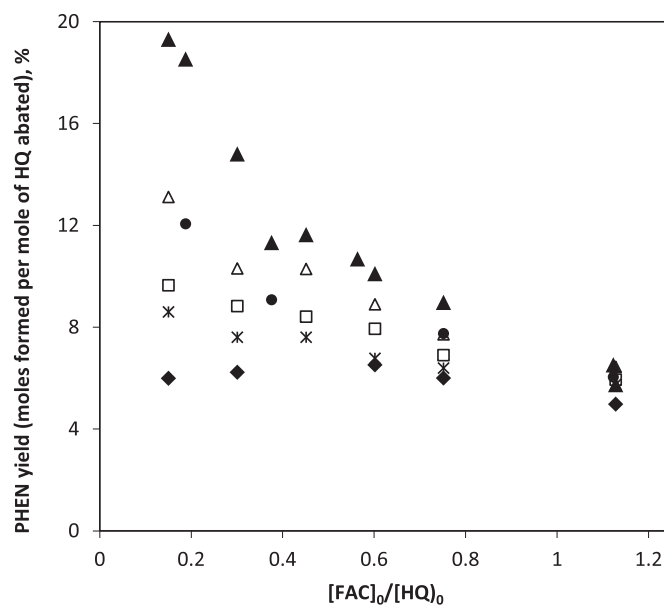
Fig. 4. Chlorination of HQ as a function of the molar $[FAC]_0/[HQ]_0$ ratios. Influence of the benzoquinone (BQ) dose on the phenol (PHEN) yield. Symbols: ▲: $[BQ]_0 = 0$; △: $[BQ]_0 = 5$ μM; ●: $[BQ]_0 = 10$ μM; □: $[BQ]_0 = 20$ μM; ✳: $[BQ]_0 = 30$ μM; ◆: $[BQ]_0 = 60$ μM; Experimental conditions: $[HQ]_0 = 62.5$ μM; BZ = 10 mM; air saturated PBS (10 mM), pH 7; $T_{exp} = 22 \pm 2$ °C; reaction time = 1.5 h.

oxidized per mole of FAC also slightly increased with increasing pH, the differences in terms of hTPA yield are negligible (Fig. 5b). In presence of oxygen as the only oxidant, an increase of pH causes a slight increase in the yield of hTPA formed from TPA-•OH (from ~28% at pH 6 to ~33% at pH 7.5, at 25 °C) (Charbouillot et al., 2011). Although k_3 also increases with increasing pH (58 M^{-1} s^{-1} at pH 7, Yamazaki and Ohnishi, 1966; 570 M^{-1} s^{-1} at pH 7.4, Eyer, 1991), which could favor the formation of $O_2^{\bullet-}$, an increase in k_7 is also expected counteracting this effect.

3.1.5. Influence of dissolved oxygen concentration

In contrast to HOCl$^{\bullet-}$ (reaction 8), the formation of $O_2^{\bullet-}$ requires the presence of oxygen (reaction 2). Hence, if this species is mainly responsible for •OH generation during HQ chlorination, the formation of hTPA or PHEN must strongly depend on the O_2 concentration. In addition, it is important to note that, in absence of other oxidants, the mechanisms of hTPA and PHEN formation (from the TPA-•OH or BZ-•OH reactions) also require the presence of O_2 (Mathews, 1980; Fang et al., 1996; Pan et al., 1993). The reactions of the radical intermediates with O_2 leading to PHEN or hTPA could also produce molar equivalents of $O_2^{\bullet-}$, which could contribute to the •OH formation by reaction 9. In absence of O_2, products different than hTPA or PHEN could be formed. All these aspects will be discussed in more detail in the section on reaction kinetics.

To investigate the effect of O_2, air saturated ($[O_2] \sim 300$ μM), oxygen saturated ($[O_2] \sim 1200$ μM) and N_2 saturated (O_2 purged by stripping with N_2) solutions containing 62.5 μM HQ were chlorinated (pH 7 and room temperature), using TPA as •OH scavenger. The results in Fig. 6, show that hTPA is not formed in absence of O_2, both hTPA concentrations (Fig. 6a) and yields (Fig. 6b) increased with increasing O_2 levels. For oxygen saturated conditions (the O_2 concentration increased four fold compared to air saturation), hTPA concentrations were 2–3 times higher and the yield increased ~ 3–4 times, the latter due to the lower efficiency of HQ abatement for increasing O_2 concentrations (Fig. 6c). Overall, an increase in O_2 favors the formation of $O_2^{\bullet-}$ through reaction 2 and, at
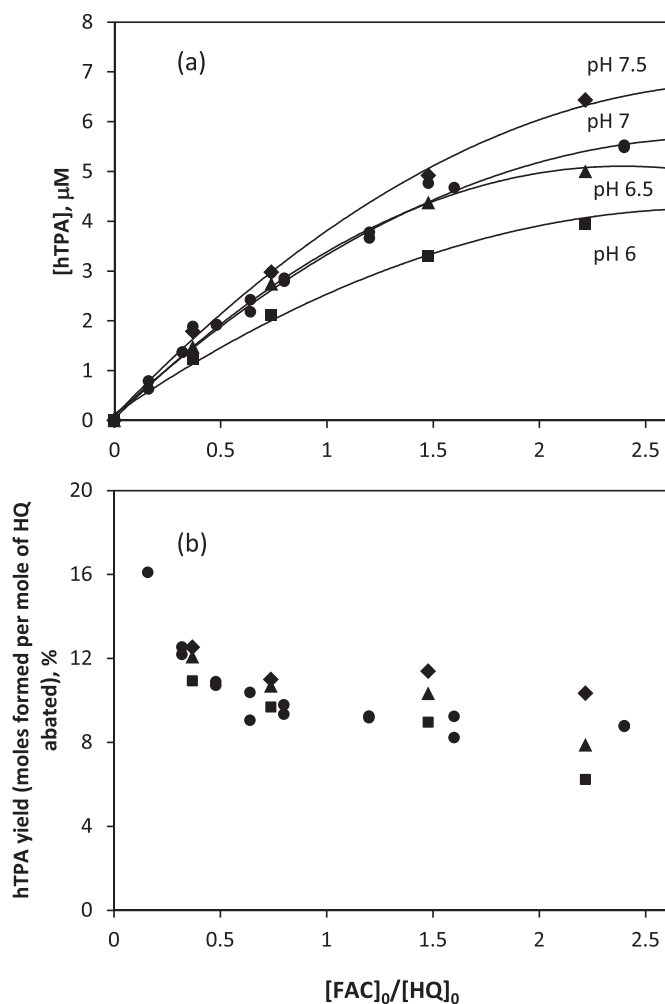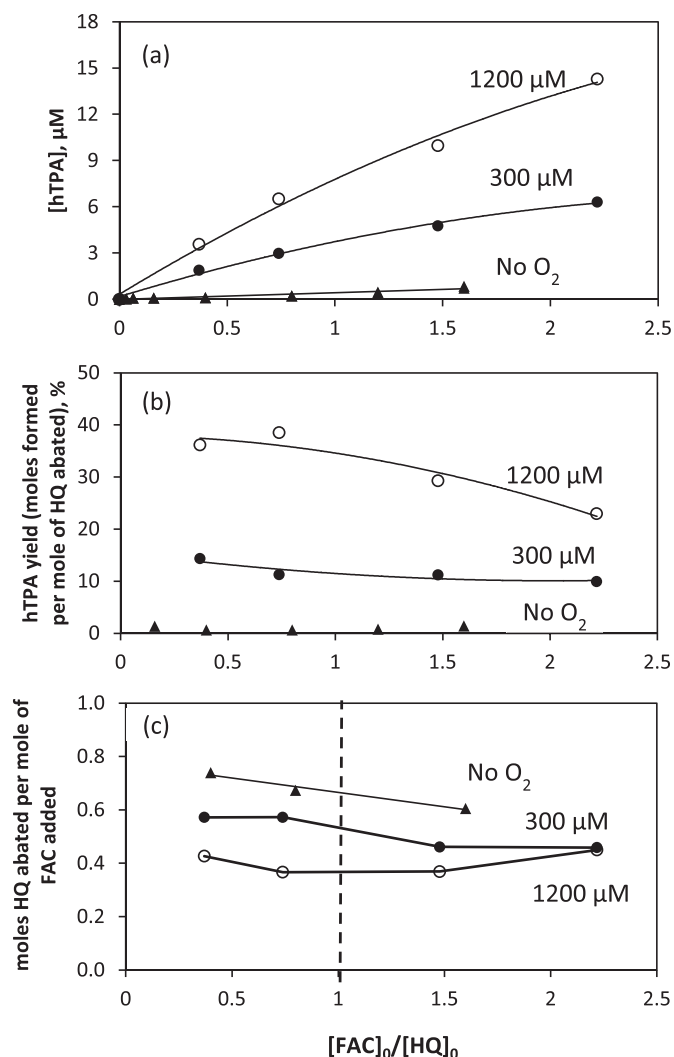
Fig. 5. Chlorination of HQ as a function of the molar $[FAC]_0/[HQ]_0$ ratios. Influence of pH on (a) hTPA formation and (b) hTPA yield. Symbols: ■: pH 6; ▲: pH 6.5; ●: pH 7; ◆: pH 7.5. Experimental conditions: $[HQ]_0 = 62.5$ μM; TPA = 4 mM; air saturated PBS (10 mM); $T_{exp} = 22 \pm 2$ °C; reaction time = 1.5 h. The lines in Fig. 5a are shown to guide the eye.

the same time, the chlorine consumption by reaction 9. From these results, it seems quite evident that $O_2^{•-}$ participates in the generation of $^{•}OH$. Moreover, the strong influence of O_2 levels on hTPA and PHEN generation would indicate that a contribution of $HOCl^{•-}$ to $^{•}OH$ production through reaction 8 is less important.

Similar results were obtained for the influence of O_2 on PHEN formation and yields when BZ was used as $^{•}OH$ scavenger. However, in this case, to avoid BZ volatilization, the level of O_2 in the samples could only be partially reduced or increased (Fig. S6, SI). The possible contribution to $^{•}OH$ formation from superoxide that can be generated from BZ-$^{•}OH$ or TPA-$^{•}OH$ reactions will also be discussed in the kinetics section.
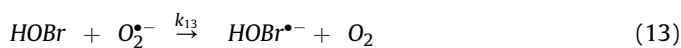
3.1.6. Bromination of hydroquinone

Similar to chlorine, bromine oxidizes HQ to BQ, with a significantly higher second order rate constant for this reaction at pH 7 compared to FAC ($k_{HOBr-HQ} = 6.4 \times 10^4$ M^{-1} s^{-1} vs $k_{FAC-HQ} = 21.6$ M^{-1} s^{-1}; Criquet et al., 2015). The second order rate constant for the reaction between HOBr and $O_2^{•-}$ (reaction 13) is also about three orders of magnitude higher than for HOCl (reaction 9) ($k_{13} = 3.5 \times 10^9$ M^{-1} s^{-1}; Schwarz and Bielski, 1986), and leads to $HOBr^{•-}$ that further evolves to $^{•}OH$ through reaction 14

Fig. 6. Chlorination of HQ as a function of the molar $[FAC]_0/[HQ]_0$ ratios. Influence of dissolved O_2 on (a) hTPA formation, (b) hTPA yield and (c) moles of HQ eliminated per mole of FAC added. Symbols: ▲: N_2 saturated (no O_2); ●: Air saturated ($[O_2] \sim 300$ μM); ○: O_2 saturated ($[O_2] \sim 1200$ μM). Experimental conditions: $[HQ]_0 = 62.5$ μM; TPA = 4 mM; PBS (10 mM) pH 7; $T_{exp} = 22 \pm 2$ °C; reaction time = 1.5 h. The lines are shown to guide the eye.

($k_{14} = 3.3 \times 10^7$ M^{-1} s^{-1} and $k_{-14} = 1.1 \times 10^{10}$ M^{-1} s^{-1}; Zehavi and Rabani, 1972), and also to Br$^{•}$ and OH$^-$ through reaction 15 ($k_{15} = 4.2 \times 10^6$ M^{-1} s^{-1} and $k_{-15} = 1.3 \times 10^{10}$ M^{-1} s^{-1}; Zehavi and Rabani, 1972; Ross et al., 1998).

$$HOBr + O_2^{•-} \xrightarrow{k_{13}} HOBr^{•-} + O_2 \tag{13}$$

$$HOBr^{•-} \underset{k_{-14}}{\overset{k_{14}}{\rightleftarrows}} {}^{•}OH + Br^- \tag{14}$$

$$HOBr^{•-} \underset{k_{-15}}{\overset{k_{15}}{\rightleftarrows}} Br^{•} + OH^- \tag{15}$$

The experiments were performed at pH 7 (PBS, 10 mM, air saturated) with 62.5 μM $[HQ]_0$, using 4 mM TPA as a scavenger and molar $[HOBr]_0/[HQ]_0$ ratios between 0 and 1.5. The apparent stoichiometry of HOBr:HQ reaction was ~1:1 (Fig. S7, SI), in agreement with Criquet et al. (2015). In these experiments hTPA was not detected. A plausible explanation for this observation could be the

much higher value of $k_{HOBr-HQ}$ compared to that of k_{FAC-HQ}, wherefore, HOBr would be quickly and totally consumed by HQ with no chance to react with $O_2^{\bullet-}$ so neither $HOBr^{\bullet-}$ nor $^\bullet OH$ would be generated in this reaction system.

3.2. $^\bullet OH$ formation from chlorination of different hydroxyphenols at pH 7

The behavior of other hydroxyphenols (CAT, RES, GAL and TAN) was investigated to explore the applicability of our findings to a wider range of compounds. Their structures and reactivities towards different species (FAC, $^\bullet OH$ and $O_2^{\bullet-}$) are summarised in Table 2. At pH 7, all of these compounds except RES lead to the formation of quinones upon chlorination and have higher FAC reactivities than HQ (Criquet et al., 2015).

The experimental procedure was the same as for HQ, i.e., chlorination in 10 mM PBS air saturated at pH 7, using 4 mM TPA as scavenger with $[CAT]_0$, $[RES]_0$, or $[GAL]_0$, being 62.5 μM and $[TAN]_0 = 6.25$ μM. Hence, DOC_0 as hydroxyphenol was 375 μM for CAT and RES, and 475 μM for GAL and TAN. Relative hTPA yields normalized to DOC_0 (%) are shown in Fig. 7a. For comparative purposes, hTPA yields corresponding to HQ_0 62.5 μM ($DOC_0 = 375$ μM) are also included, and were much higher than for the rest of the tested compounds (squares, right Y-axis in Fig. 7a). In absence of FAC (control runs), formation of hTPA was negligible.

As expected, hTPA was not formed when RES was chlorinated (stars in Fig. 7a). Unlike the other selected hydroxyphenols, due to the m-position of the two OH substituents, RES chlorination proceeds through EAS, with chlorine addition, instead of ET (Criquet et al., 2015). Since there is no quinone/semiquinone formation, neither $O_2^{\bullet-}$ nor $HOCl^{\bullet-}$ can be generated. In contrast, for CAT, GAL and TAN, formation of hTPA was detected, although the yields were significantly lower than for HQ. Again, in line to what was proposed in the case of HQ bromination, a possible explanation could be the higher reactivity of these o-hydroxyphenols with FAC compared to HQ (Table 2). Since FAC is consumed more quickly, its reaction with $O_2^{\bullet-}$ can take place to a much lower extent.

Previously, it was shown that the presence of borate buffer decreased the reactivity of o-hydroxyphenols towards chlorine through the formation of a borate complex (Criquet et al., 2015). To test if the reactivity of these compounds with chlorine is a key parameter for $O_2^{\bullet-}$ formation, solutions containing 60 μM CAT were chlorinated at pH 7 in 10 mM PBS, pH 8 in 25 mM PBS and pH 8 in 50 mM borate buffer with 4 mM TPA as $^\bullet OH$ scavenger. Fig. 7b shows that the presence of borate leads to a much higher normalized hTPA yield. This supports the hypothesis, that the rate of reaction 7 is important for generation of $^\bullet OH$ through reaction 9.

Taking into account the complexity of these reaction systems, the reactivity between FAC and the hydroxyphenol (reaction 7) is probably not the only factor affecting $^\bullet OH$ formation. For example, both the relative position of the OH groups and the presence of electron donating/withdrawing groups on the aromatic ring can affect the standard reduction potentials (E^0) of the quinone/semiquinone pairs and, therefore, reaction 2 and the stability of $O_2^{\bullet-}$ (Song and Buettner, 2010). To test this, methylhydroquinone (MeHQ), with higher electron donating properties than HQ due to the presence of the methyl group, was chlorinated at pH 7 alone ($[MeHQ]_0$ 60 μM) or in combination with HQ ($[MeHQ]_0 = [HQ]_0 = 30$ μM), and the concentration of HQ, MeHQ and hTPA were determined. Although the reactivity of MeHQ towards FAC was higher than for HQ as expected (see Fig. S8, SI), the hTPA yields were very similar and close to $[HQ]_0$ 60 μM (Fig. S8, SI). These results can be explained by the influence of the methyl group on E^0 (quinone/semiquinone) and hence the ratio of k_2/k_{-2}. For MeHQ, $k_2 = 1.1 \times 10^6$ $M^{-1}s^{-1}$ and $k_2/k_{-2} = 1.4 \times 10^{-3}$, whereas for
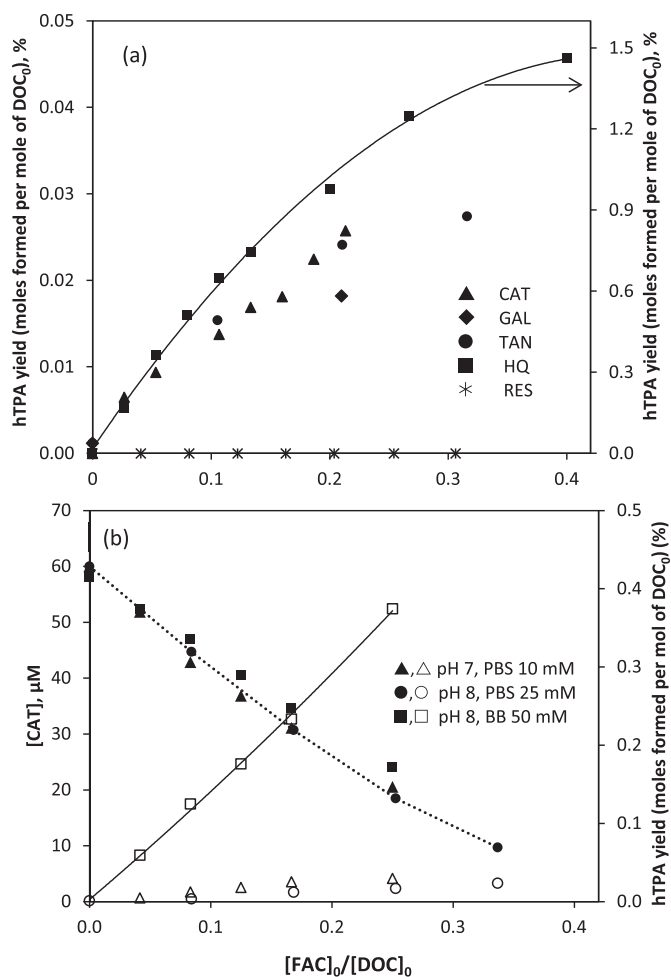

Fig. 7. (a) Chlorination of the selected hydroxyphenols. Yields of hTPA (moles formed per mole of DOC_0) for different molar $[FAC]_0/[DOC]_0$ ratios. Experimental conditions: DOC_0 (HQ) = DOC_0 (CAT) = 375 μM; DOC_0 (GAL) = DOC_0 (TAN) = 475 μM; TPA 4 mM; air saturated PBS (10 mM); pH 7; T = 22 ± 2 °C; contact time = 1.5 h. (b) Influence of the presence of borate buffer (BB) on hTPA formation (open symbols) from chlorination of CAT (closed symbols). Experimental conditions: DOC_0 (CAT) = 360 μM; TPA 4 mM; air saturated; T = 22 ± 2 °C; reaction time = 1.5 h (pH 7) and 12 h (pH 8). The lines are shown to guide the eye.

HQ $k_2 = 5 \times 10^4$ $M^{-1}s^{-1}$ and $k_2/k_{-2} = 5 \times 10^{-5}$ (Song and Buettner, 2010). This means that the presence of the methyl group favors the formation/stabilization of $O_2^{\bullet-}$ counteracting the negative effect of its higher reactivity towards FAC.

3.3. $^\bullet OH$ formation from chlorination of different NOM extracts at pH 7

The formation of $^\bullet OH$ during the chlorination of NOM extracts (SRHA, SRFA, PLFA and NL-NOM; Table S1, SI) was investigated in presence of TPA, and the formation of hTPA was measured after 72 h. The $[DOC]_0$ of the NOM extracts was 375 μM (SRHA), 392 μM (SRFA), 442 μM (PLFA) and 248 μM (NL-NOM). The specific chlorine demand of each extract (pH 7, 72 h contact time) was determined, and resulted to be 0.49, 0.34, 0.38 and 0.36 moles of FAC per mole of DOC_0 for SRHA, SRFA, PLFA and NL-NOM, respectively (Fig. S9, SI).

The DOC_0-normalized yields of hTPA (mol/mol, %) are shown in Fig. 8 as a function of the specific chlorine dose. The maximum hTPA yields followed the order PLFA (0.3) < SRFA (1.1) < SRHA (1.6) < NL-NOM (2.0). They were achieved for specific chlorine doses slightly higher than the corresponding specific chlorine
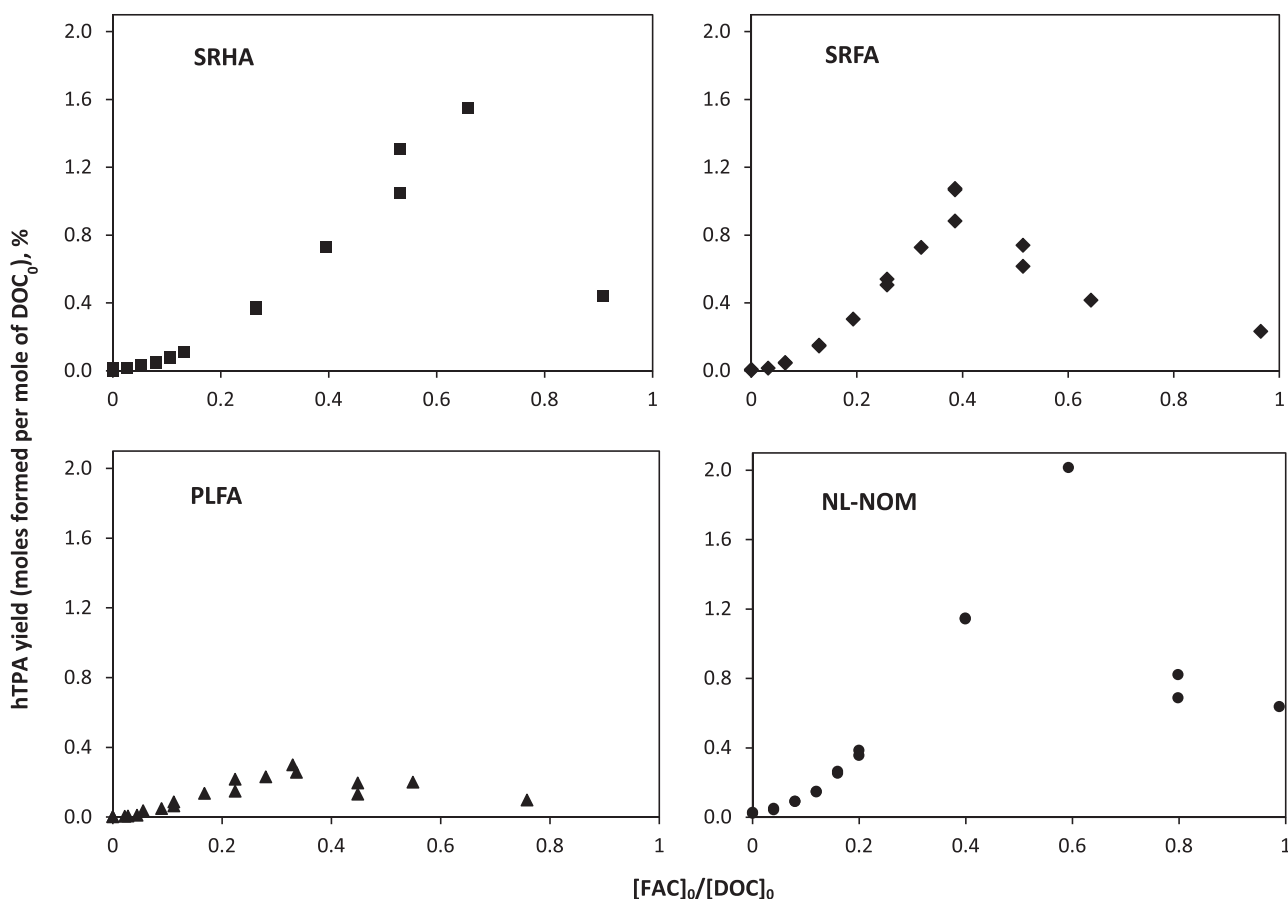
Fig. 8. DOC-normalized yields of hTPA from the chlorination of the selected NOM extracts as a function of the molar $[FAC]_0/[DOC]_0$ ratio. Experimental conditions: $[DOC-SRHA]_0 = 375$ μM; $[DOC-SRFA]_0 = 392$ μM; $[DOC-PLFA]_0 = 442$ μM; $[DOC-NL-NOM]_0 = 248$ μM; TPA = 4 mM; air saturated PBS (10 mM), pH 7; $T_{exp} = 22 \pm 2$ °C; reaction time = 72 h. SRHA: Suwannee River Humic Acid; SRFA: Suwannee River Fulvic Acid; PLFA: Pony Lake Fulvic Acid; NL-NOM: Nordic Lake NOM.

demands, which is due to some FAC consumption by TPA under these conditions. After reaching these maxima, higher chlorine doses led to lower hTPA yields probably due to its reaction with FAC ($k_{FAC-hTPA} = 0.15$ M^{-1} s^{-1} at pH 7 and 25 °C; this study). It has to be mentioned that hTPA was also formed in very low concentrations in absence of FAC (control runs). This means that the NOM extracts can generate $^{\bullet}$OH in aqueous solution in the dark. This effect was also observed previously during aeration of different anoxic lake waters and attributed to the development of Fenton-like reactions that involve HQ/SQ$^{\bullet-}$ and/or Fe(II) (Minella et al., 2015). After 72 h, the hTPA yields (mol hTPA/mol DOC$_0$, %) of the control samples were about 2 orders of magnitude smaller, but following the same sequence as for chlorination (0.002 (PLFA) < 0.006 (SRFA) < 0.02 (SRHA) < 0.03 (NL-NOM)).

Among the selected extracts, PLFA (autochthonous NOM) presents the lowest SUVA$_{254}$, EDC, aromatic C and phenolic content (Table S1 in SI, and references therein). PLFA has the lowest $^{\bullet}$OH yield, which seems to indicate that phenolic structures in NOM are involved in $^{\bullet}$OH formation during chlorination of NOM. With the exception of PLFA, the DOC-normalized hTPA yields for the selected NOMs were close or even higher than for HQ (Fig. 7a). Thus, in case hydroxyphenols in NOM are the main source of $^{\bullet}$OH during chlorination, HQ moieties with higher $^{\bullet}$OH formation potential than HQ must be present. This points towards the presence of HQ-like structures in NOM with lower reactivity with FAC than HQ, thus allowing FAC to react with O$_2^{\bullet-}$. Alternatively, this could be

explained by the presence or formation of quinone structures with higher k_2 and k_2/k_{-2} values than HQ (that is, structures with low E^0 quinone/semiquinone) favoring the formation/stabilization of O$_2^{\bullet-}$. Also, NOM moieties different from phenols could be responsible for $^{\bullet}$OH formation upon chlorination. Based on the information in Table S1 (SI), *N*-containing structures are probably not involved, since PLFA has the lowest $^{\bullet}$OH formation potential, but contains 4−10 times more N than the other extracts. And finally, the higher the iron content, the higher the amount of $^{\bullet}$OH produced. To this end, a study by Santana-Casiano et al. (2010) carried out in seawater demonstrated that Fe(III)-CAT complexes are formed, followed by Fe(III) reduction to Fe(II) and CAT oxidation to SQ$^{\bullet-}$, with generation of O$_2^{\bullet-}$. Hence, the enhancement of $^{\bullet}$OH formation due to iron complexes in NOM cannot be disregarded.

Water from Lake Greifensee (LG, Switzerland) was also chlorinated (DOC$_0$ 250 μM; pH 7.85 after the addition of TPA; specific chlorine demand 0.22 moles of FAC per mole of DOC), and the formation of hTPA was measured. In absence of FAC (control runs), after 72 h contact time, the molar DOC-normalized hTPA yield (%) was <0.003. The results obtained (see Fig. S10, SI), indicate that DOM in LG water was capable of producing $^{\bullet}$OH when chlorinated. However, the maximum DOC-normalized hTPA formation was low, ~0.1% mol (mol DOC$_0$)$^{-1}$, similar to PLFA (also of autochthonous origin; Wenk et al., 2011), and more than ten times lower than for HQ and the other investigated NOM extracts.
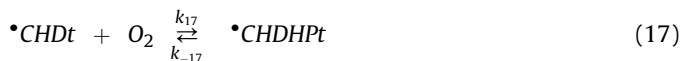
3.4. Modelling of the kinetics of $^\bullet OH$ formation during HQ chlorination at pH 7

In the last part of the study, the formation of $^\bullet OH$ during HQ chlorination at pH 7 has been modeled based on the experimental results and the kinetic data available. All the reactions considered and their rate constants are compiled in Table S3 in SI. The kinetic model is based on reactions (1)–(3) and (7) assuming values of 10^{-7} and 10^7 M^{-1} s^{-1} for k_1 and k_{-1}, respectively ($K_1 = 10^{-14}$; Eyer, 1991). At pH 7, k_5 is very low (Sheng et al., 2014), and from equilibrium 4 the contribution of reaction 6 can be disregarded (see below). Also, due to the strong effect of O$_2$ concentration on hTPA and PHEN formation (see section 3.1.5), keeping in mind that reactions 8 and 10 are oxygen-independent, the contributions of these reactions to $^\bullet OH$ formation is expected to be minimal and they have not been considered. For reaction 7, according to the experimental results a molar stoichiometry 2:1 FAC:HQ has been assumed (see Fig. 1b; and also Fig. S11, SI).

According to the pKa of FAC (7.49, equilibrium 12), at pH 7, the molar fractions of HOCl and ClO$^-$ are 0.756 and 0.244, respectively. Since ClO$^-$ does not react with O$_2^{\bullet-}$ (Long and Bielski, 1980), reaction 9 can be rewritten in terms of FAC with an apparent second order rate constant $k_{9b} = 5.6 \times 10^6$ M^{-1} s^{-1} at pH 7 (Long and Bielski, 1980):
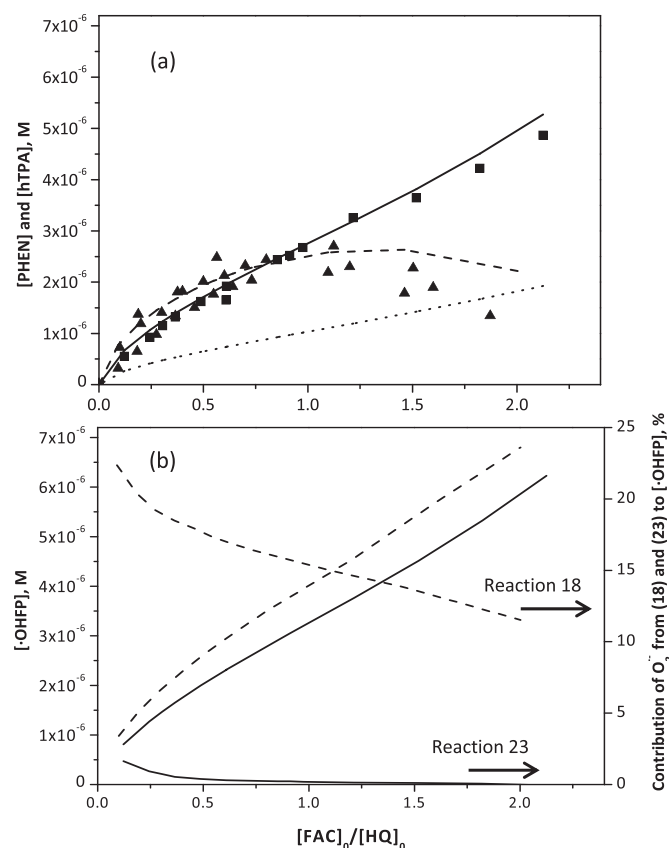
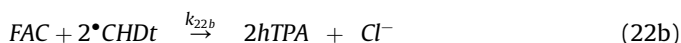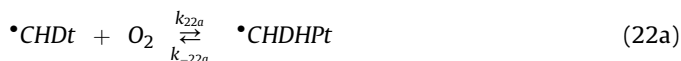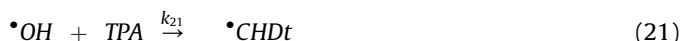$$FAC + O_2^{\bullet-} \xrightarrow{k_{9b}} Cl^- + {}^\bullet OH + O_2 \tag{9b}$$
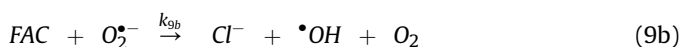
In presence of BZ as $^\bullet OH$ scavenger, the following reactions have been considered (Pan et al., 1993; Fang et al., 1995):

$$^\bullet OH + BZ \xrightarrow{k_{16}} {}^\bullet CHDt \tag{16}$$

$$^\bullet CHDt + O_2 \underset{k_{-17}}{\overset{k_{17}}{\rightleftarrows}} {}^\bullet CHDHPt \tag{17}$$

$$^\bullet CHDHPt \xrightarrow{k_{18}} PHEN + O_2^{\bullet-} \tag{18}$$

$$^\bullet CHDHPt \xrightarrow{k_{19}} P1BZ \tag{19}$$

where $^\bullet CHDt$ is a cyclohexadienyl-type radical intermediate ($k_{16} = 7.8 \times 10^9$ M^{-1} s^{-1}; Buxton et al., 1988), $^\bullet CHDHPt$ the cyclohexadienylhydroperoxide-type radical ($k_{17} = 3.1 \times 10^8$ M^{-1} s^{-1}, $k_{-17} = 1.2 \times 10^4$ s^{-1}; Fang et al., 1995), and P1BZ another final product other than PHEN. Since the rate constant of $^\bullet CHDHPt$ decrease is 800 s^{-1} (Fang et al., 1995), by assuming a yield of 85% for PHEN and 15% for P1BZ (Dong and Rosario-Ortiz, 2012), k_{18} and k_{19} values have been assumed to be 680 s^{-1} and 120 s^{-1}, respectively.

In presence of TPA as $^\bullet OH$ scavenger, the following reactions have been considered (Fang et al., 1996):

$$^\bullet OH + TPA \xrightarrow{k_{20}} P1TPA \tag{20}$$

$$^\bullet OH + TPA \xrightarrow{k_{21}} {}^\bullet CHDt \tag{21}$$

$$^\bullet CHDt + O_2 \underset{k_{-22a}}{\overset{k_{22a}}{\rightleftarrows}} {}^\bullet CHDHPt \tag{22a}$$

$$FAC + 2{}^\bullet CHDt \xrightarrow{k_{22b}} 2hTPA + Cl^- \tag{22b}$$

Fig. 9. Chlorination of HQ as a function of the molar [FAC]$_0$/[HQ]$_0$ ratios. (a) Experimental (symbols) and calculated (lines) final concentrations of PHEN (from BZ) and hTPA (from TPA). Symbols: ■: hTPA; ▲: PHEN; Lines: (——) hTPA considering reaction 22b and assuming $k_{22b} = k_{21}$; (.....) hTPA without participation of 22b; (- - -) PHEN. (b) Modelling of total $^\bullet OH$ formation potential ($^\bullet OHFP$) and % contribution of O$_2^{\bullet-}$ generated from reactions 18 and 23 (optimized $k_{22b} = 10^8$ M^{-1}s^{-1}). Lines: (——) using TPA as $^\bullet OH$ scavenger and considering reaction (22b); (- - -) using BZ as $^\bullet OH$ scavenger. Conditions: [HQ]$_0$ = 62.5 μM; TPA = 4 mM; BZ = 10 mM; PBS (10 mM) pH 7 air sat.; T$_{exp}$ = 22 ± 2 °C; T$_{model}$ = 25 °C; reaction time = 1.5 h.

$$^\bullet CHDHPt \xrightarrow{k_{23}} hTPA + O_2^{\bullet-} \tag{23}$$

$$^\bullet CHDHPt \xrightarrow{k_{24}} P2TPA \tag{24}$$

where P1TPA and P2TPA represent products different from hTPA and $^\bullet CHDt$ the cyclohexadienyl-type radical formed when $^\bullet OH$ was added to the *ortho* position of TPA. From the overall rate constant of the TPA - $^\bullet OH$ reaction (4.4×10^9 M^{-1}s^{-1}, Page et al., 2010) and the corresponding yields (85% for $^\bullet CHDt$ and 15% for P1TPA; Fang et al., 1996), values of 0.66×10^9 M^{-1}s^{-1} and 3.74×10^9 M^{-1} s^{-1} have been assigned for k_{20} and k_{21}, respectively. According to Fang et al. (1995), $k_{22a} = 1.6 \times 10^7$ M^{-1} s^{-1} and $k_{-22a} = 3.4 \times 10^3$ s^{-1}, whereas the rate constant of $^\bullet CHDHPt$ decomposition (reactions 23 and 24) is 390 s^{-1}. By considering a global yield of 30% for hTPA and 55% for P2TPA, k_{23} and k_{24} values were assumed to be 138 s^{-1} and 252 s^{-1}, respectively.

Similarly to what was observed by Fang et al. (1995) during the TPA -$^\bullet OH$ reaction in presence of IrCl$_6^{2-}$, another possible scenario in which FAC can also oxidize $^\bullet CHDt$ directly and irreversibly to hTPA (without formation of $^\bullet CHDHPt$ or O$_2^{\bullet-}$) has been considered (reaction 22b), initially assuming the same rate constant for this reaction as for reaction 21, that is, $k_{22b} = 3.74 \times 10^9$ M^{-1}s^{-1}.

Finally, the reactions of FAC and •OH with other compounds have also been introduced in the mechanism (reactions 25−28 and 29−34, respectively. See Table S3, SI). However, since at the experimental conditions applied in this study $f(•OH) \geq 0.95$ for TPA and BZ (Table S1, SI), reactions 29−34 are expected to be negligible.

A comparison between experimental and modeled final concentrations of PHEN and hTPA for chlorination of HQ 62.5 μM for different $[FAC]_0/[HQ]_0$ molar ratios is shown in Fig. 9a (symbols: experimental results, lines: model calculations). When TPA was used as •OH scavenger the two possible scenarios (that is, without/with participation of 22b) were considered, in the latter case initially assuming $k_{22b} = k_{21}$ as indicated before. In Fig. 9a, a good agreement between experimental and modeled data is observed for PHEN, whereas in the case of hTPA its formation through the $O_2^{•-}$ dependent mechanism (reactions 22a and 23, without participation of 22b), clearly underestimate the experimental values (Fig. 9a, dotted line). In contrast, when reaction 22b is also considered, the experimental/calculated hTPA agree within the experimental errors (Fig. 9a, solid line).

To further investigate the role of reaction 22b, the two scenarios were tested for lower HQ_0 and FAC_0 conditions, again initially assuming $k_{22b} = k_{21}$. From the evolution of experimental and modeled hTPA as a function of the FAC concentration (see Fig. S12, SI) it seems that for $[FAC]_0 > 1$ mg L^{-1} reaction 22b (solid lines) is the main source of hTPA, and hence ~ 0.85 moles of hTPA are formed per mole of •OH generated. At lower FAC doses (<1 mg/L) the participation of the O_2-based mechanism (reactions 22a and 23) increases, with hTPA yields in the range of 30%−85%. The fact that in presence of FAC the yield of hTPA formation from the TPA -•OH reaction is higher than 30% would explain why the experimental concentrations and yields of PHEN and hTPA were similar for $[FAC]_0/[HQ]_0$ molar ratios ≤ 1 (see Fig. 2). The value for k_{22b} was optimized by various model calculations to minimize the differences between experimental and calculated hTPA for different initial HQ and FAC concentrations. The optimized value is $k_{22b} = 10^8$ M^{-1}s^{-1} (see Fig. S13, SI) which was then applied for all model calculations.

In any case, the yields of both hTPA (from the TPA -•OH reaction) and PHEN (from the BZ -•OH reaction) are lower than 100%. This implies that the total formation potential of •OH (•OHFP), is higher than the measured PHEN or hTPA concentrations. The •OHFPs of HQ 62.5 μM as a function of $[FAC]_0/[HQ]_0$ at pH 7 in presence of BZ 10 mM or TPA 4 mM were modeled. As shown in Fig. 9b, the total production of •OH in presence of BZ (dashed line) is higher than for

TPA (solid line), attributable to the $O_2^{•-}$ generated through reaction 18. The calculated relative contribution (%) of $O_2^{•}$ formed from reactions 18 or 23 to •OHFP, is also indicated in Fig. 9b (reaction 18: dashed line; reaction 23: solid line). For TPA this contribution was minimal (lower than 1%), whereas for BZ it decreased from ~22% to 10% as the FAC dose increased.

At the conditions tested and as expected, the introduction of equilibrium 4 and reaction 6 in the mechanism did not cause any change. The presence of FAC and/or BQ in the reaction medium together with the low concentration of $O_2^{•-}$ and $HO_2^{•-}$ in solution (~10^{-11} and 10^{-13} M, respectively) prevent the formation of HO_2^{-} through 6.

The effect of the initial HQ concentration on the experimental hTPA yield (that is, for a given $[FAC]_0/[HQ]_0$ the hTPA yield decreases with increasing $[HQ]_0$, see Fig. 3) is also well predicted by the proposed mechanisms (Fig. S14, SI).

The negative effect of BQ on •OHFP experimentally observed (see Fig. 4), is also corroborated by this mechanism. As an example, Fig. S15 (SI) shows the modeled reduction of the •OHFP (%) during the chlorination of HQ (62.5 μM, pH 7, air saturated) in presence of different concentrations of BQ, with 4 mM TPA or 10 mM BZ as scavengers. As observed, the higher the initial BQ concentration, the higher the reduction of the •OHFP. For a given $[BQ]_0$, this effect is attenuated by the BQ formed from HQ chlorination as the $[FAC]_0$ increases. Thus, the formation of BQ from the HQ - chlorine reaction seems to be the main reason why, for a given $[HQ]_0$, •OHFP (and hence hTPA or PHEN yields) decreases as the dose of FAC increases, BQ acting as $O_2^{•-}$ scavenger.

Finally, the role of dissolved O_2 on •OH generation and hence hTPA formation is also well predicted by the proposed mechanisms, as shown in Fig. S16 (SI) for the experiments performed using TPA as •OH scavenger. Fig. S16a (SI) shows that for O_2-saturated conditions ($[O_2] = 1200$ μM) reaction 22b seems to be the main source of hTPA, although in this case the model for the optimized k_{22b} value (dashed line) slightly underestimates the actual hTPA concentrations. However, the model fit is still very good considering the significant number of reactions. Fig. S16b (SI) shows the •OHFP predicted at air-saturated conditions ($[•OHFP]_{air\ sat.}$, being $[O_2]_{air\ sat} = 300$ μM) for HQ 62.5 μM chlorination as a function of FAC dose, together with the evolution of the predicted $[•OHFP]/[•OHFP]_{air\ sat.}$ ratio for different O_2 concentrations. As observed, for dissolved oxygen concentrations 50, 100 and 200 μM, that is, $[O_2]/[O_2]_{air\ sat}$ values 0.17, 0.33 and 0.67, respectively, the $[•OHFP]/[•OHFP]_{air\ sat.}$ is ~ 0.21, 0.39 and 0.71, whereas at O_2 saturation conditions ($[O_2]/$
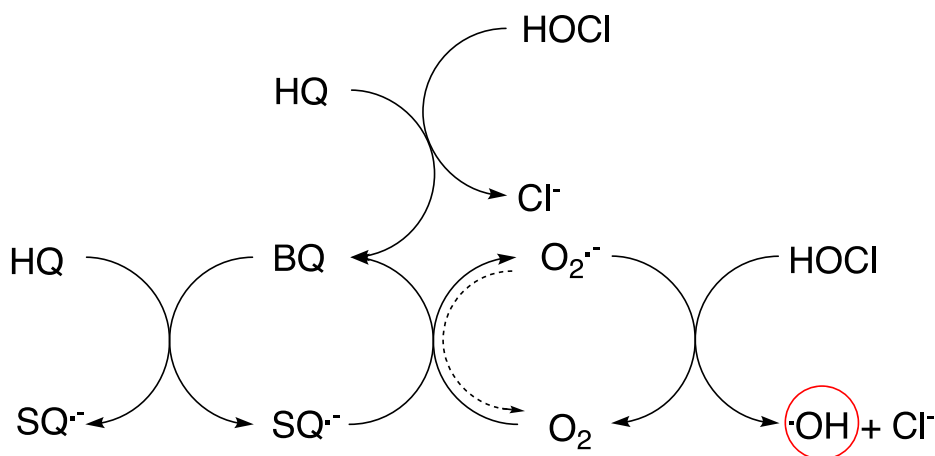

Fig. 10. Hypothetic mechanism for the formation of hydroxyl radical induced by the hydroquinone-HOCl reaction. HQ: hydroquinone; BQ: benzoquinone; SQ$^{•-}$: Semiquinone radical.

$[O_2]_{air\ sat} = 4$), it results to be 2.5–3. In agreement with the experimental results, the relationship between O_2 concentration and the $^\bullet$OHFP is not linear.

Based on the findings of this study, a mechanism for $^\bullet$OH formation during HQ chlorination is proposed in Fig. 10.

The mechanism depicted in Fig. 10 shows that in a first step BQ is formed from the reaction of HQ with chlorine. HQ and BQ react to two semiquinone radicals, which then react with molecular oxygen to form superoxide radical. Finally, HOCl reacts with superoxide to form hydroxyl radical. BQ can also react with superoxide, leading back to molecular oxygen. Therefore, the BQ concentration can affect the hydroxyl radical yield significantly.

4. Conclusions

- With the aid of different scavengers the generation of hydroxyl radical ($^\bullet$OH) during the chlorination of *o-* and *p*-hydroxyphenols at neutral pH conditions has been demonstrated.
- The mechanism of $^\bullet$OH generation requires the formation of semiquinones capable of reducing dissolved oxygen to superoxide radical, which further reacts with HOCl to $^\bullet$OH.
- For *p*-hydroxyphenols the $^\bullet$OH yield (in terms of moles formed per mole of DOC_0) was clearly higher and comparable to that of SRHA, SRFA and NL NOM, all these extracts presenting high electron donating capacities.
- According to the results obtained, a low reactivity towards chlorine and a high presence/formation of quinone structures with low E^0 favor the formation/stabilization of $O_2^{\bullet-}$, thereby increasing the potential of $^\bullet$OH formation during the chlorination of NOM.
- From the combination of experimental results with kinetic modelling, a mechanism for hydroquinone chlorination at pH 7 has been proposed, which can explain the findings well.

Declaration of competing interest

The authors declare that they have no known competing financial interests or personal relationships that could have appeared to influence the work reported in this paper.

Appendix A. Supplementary data

Supplementary data to this article can be found online at https://doi.org/10.1016/j.watres.2020.115691.

References

Aeschbacher, M., Graf, C., Schwarzenbach, R.P., Sander, M., 2012. Antioxidant properties of humic substances. Environ. Sci. Technol. 46, 4916–4925. https://doi.org/10.1021/es300039h.

Amels, P., Elias, H., Wannowius, K.-J., 1997. Kinetics and mechanism of dimethyl sulfide by hydroperoxides in aqueous medium. J. Chem. Soc., Faraday Trans. 93, 2537–2544. https://doi.org/10.1039/A700722A.

Bardouki, H., Barcellos da Rosa, M., Mihalopoulos, N., Palm, W.U., 2002. Zetzsch. Kinetics and mechanism of the oxidation of simethylsulfoxyde (DMSO) and methanesulfinate (MSI⁻) by OH radicals in aqueous medium. C. Atmos. Environ. 36, 4627–4634. https://doi.org/10.1016/S1352-2310(02)00460-0.

Bielski, B.H.J., Cabelli, D.E., Arudi, R.L., Ross, A.L., 1985. Reactivity of HO₂/O₂- radicals in aqueous solution. J. Phys. Chem. Ref. Data 14, 1041–1100. https://doi.org/10.1063/1.555739.

Bond, T., Goslan, E.H., Parsons, S.A., Jefferson, B., 2012. A critical review of trihalomethane and haloacetic acid formation from natural organic matter surrogates. Environ. Technol. Rev. 1, 93–113. https://doi.org/10.1080/09593330.2012.705895.

Bors, W., Michel, C., 1999. Antioxidant capacity of flavonols and gallate esters : pulse radiolysis studies. Free Radic. Biol. Med. 27, 1413–1426. https://doi.org/10.1016/s0891-5849(99)00187-2.

Bulman, D.V., Mezyk, S.P., Remucal, C.K., 2019. The impact of pH and irradiation wavelength on the production of reactive oxidants during chlorine photolysis. Environ. Sci. Technol. 53, 4450–4459. https://doi.org/10.1021/acs.est.8b07225.

Buxton, G.V., Greenstock, C.L., Helman, W.P., Ross, A.B., 1988. Critical review of rate constants for reactions of hydrated electrons, hydrogen atoms and hydroxyl radicals (·OH/·O-) in aqueous solution. J. Phys. Chem. Ref. Data 17, 513–886. https://doi.org/10.1063/1.555805.

Candeias, L.P., Patel, K.B., Stratford, M.R.L., Wardman, P., 1993. Free hydroxyl radicals are formed on reaction between the neutrophil-derived species superoxide anion and hypochlorous acid. Federation of European Biochemical Societies 333, 151–153. https://doi.org/10.1016/0014-5793(93)80394-a.

Cederbaum, A.I., Qureshi, A., Cohen, G., 1983. Production of formaldehyde and acetone by hydroxyl-radical generating systems during the metabolism of tertiary butyl alcohol. Biochem. Pharmacol. 32, 3517–3524. https://doi.org/10.1016/0006-2952(83)90297-6.

Charbouillot, T., Brigante, M., Mailhot, G., Maddigapu, P.R., Minero, C., Vione, D., 2011. Performance and selectivity of the terephthalic acid probe for ·OH as a function of temperature, pH and composition of atmospherically relevant aqueous media. J. Photochem. Photobiol. Chem. 222, 70–76. https://doi.org/10.1016/j.jphotochem.2011.05.003.

Criquet, J., Rodríguez, E.M., Allard, S., Wellauer, S., Salhi, E., Joll, C.A., von Gunten, U., 2015. Reaction of bromine and chlorine with phenolic compounds and natural organic matter extracts- electrophilic aromatic substitution and oxidation. Water Res. 85, 476–486. https://doi.org/10.1016/j.watres.2015.08.051.

Deister, U., Warneck, P., Wurzinger, C., 1990. OH radicals generated by NO₃ photolysis in aqueous solution: competition kinetics and a study of the reaction OH + CH₂(OH)SO₃. Ber. Bunsenges. Phys. Chem. 94, 594–599. https://doi.org/10.1002/bbpc.19900940512.

Dong, M.M., Rosario-Ortiz, F.L., 2012. Photochemical formation of hydroxyl radical from effluent organic matter. Environ. Sci. Technol. 46, 3788–3794. https://doi.org/10.1021/es2043454.

Dwibedy, P., Dey, G.R., Naik, D.B., Kishore, K., Moorthy, P.N., 1999. Pulse radiolysis studies on redox reactions of gallic acid : One electron oxidation of gallic acid by gallic acid-OH adduct. Phys. Chem. Chem. Phys. 1, 1915–1918. https://doi.org/10.1039/A809147A.

Eyer, P., 1991. Effects of superoxide dismutase on the autoxidation of 1,4-hydroquinone. Chem.-Biol. Interactions 80, 159–176. https://doi.org/10.1016/0009-2797(91)90022-y.

Fang, X., Pan, X., Rahmann, A., Schuchmann, H.P., von Sonntag, C., 1995. Reversibility in the reaction of cyclohexadienyl radicals with oxygen in aqueous solution. Chem. Eur J. 7, 423–429. https://doi.org/10.1002/chem.19950010706.

Fang, X., Mark, G., von Sonntag, C., 1996. OH radical formation by ultrasound in aqueous solutions Part I: the chemistry underlying the terephthalate dosimeter. Ultrason. Sonochem. 3, 57–63. https://doi.org/10.1016/1350-4177(95)00032-1.

Flyunt, R., Leitzke, A., Mark, G., Mvula, E., Reisz, E., Schick, R., von Sonntag, C., 2003. Determination of ·OH, O₂⁻, and hydroperoxide yields in ozone reactions in aqueous solution. J. Phys. Chem. B 107, 7242–7253. https://doi.org/10.1021/jp022455b.

Gallard, H., von Gunten, U., 2002. Chlorination of phenols: kinetics and formation of chloroform. Environ. Sci. Technol. 36, 884–890. https://doi.org/10.1021/es010076a.

Gurol, M.D., Vatistas, R., 1987. Photolytic ozonation of phenols. Water Sci. Technol. 19, 1177–1180. https://doi.org/10.2166/wst.1987.0005.

Hand, V.C., Margerum, D.W., 1983. Kinetics and mechanism of the decomposition of dichloramine in aqueous solution. Inorg. Chem. 11, 1449–1456. https://doi.org/10.1021/ic00152a007.

Heeb, M.B., Kristiana, I., Trogolo, D., Arey, J.S., von Gunten, U., 2017. Formation and reactivity of inorganic and organic chloramines and bromamines during oxidative water treatment. Water Res. 110, 91–101. https://doi.org/10.1016/j.watres.2016.11.065.

Huisman, A., van de Wiel, A., Rabelink, T.J., van Faasen, E.E., 2004. Wine polyphenols and ethanol do not significantly scavenge superoxide nor affect endothelial nitric oxide production. J. Nutr. Biochem. 15, 426–432. https://doi.org/10.1016/j.jnutbio.2004.01.006.

James, T.H., Snell, J.M., Weissberger, A., 1938. Oxidation Processes. XII. The autoxidation of hydroquinone and of the mono-, di- and trimethylhydroquinones. J. Am. Chem. Soc. 60, 2084–2093. https://doi.org/10.1021/ja01276a020.

Jayson, G.G., Parsons, B.J., Swallow, A.J., 1973. Some simple, highly reactive, inorganic chlorine derivatives in aqueous solution. Their formation using pulses of radiation and their role in the mechanism of the Fricke dosimeter. J. Chem. Soc., Faraday Trans. 1 (69), 1597–1607. https://doi.org/10.1039/F19736901597.

Lee, Q., Westerhoff, P., Croué, J.P., 2007. Dissolved organic nitrogen as a precursor for chloroform, dichloroacetonitrile, N-nitrosodimethylamine and trichloromethane. Environ. Sci. Technol. 41, 5485–5490. https://doi.org/10.1021/es070411g.

Le Roux, J., Nihemaiti, M., Croue, J.P., 2016. The role of aromatic precursors in the formation of haloacetamides by chloramination of dissolved organic matter.

Water Res. 88, 371–379. https://doi.org/10.1016/j.watres.2015.10.036.

Long, C.A., Bielski, B.H.J., 1980. Rate of reaction of superoxide radical with chloride-containing species. J. Phys. Chem. 84, 557–558. https://doi.org/10.1021/j100442a023.

Mathews, R.W., 1980. The radiation chemistry of the terephthalate dosimeter. Radiat. Res. 83, 27–41. https://doi.org/10.2307/3575256.

Minella, M., De Laurentis, E., Maurino, V., Minero, C., Vione, D., 2015. Dark production of hydroxyl radicals by aeration of anoxic lake water. Sci. Total Environ. 527–528, 322–327. https://doi.org/10.1016/j.scitotenv.2015.04.123.

Nadezhdin, A.D., Dunford, H.B., 1979. The oxidation of ascorbic acid and hydroquinone by perhydroxyl radicals. A flash photolysis study. Can. J. Chem. 57, 3017–3022. https://doi.org/10.1139/v79-491.

Önnby, L., Salhi, E., McKay, G., Rosario-Ortiz, F.L., von Gunten, U., 2018. Ozone and chlorine reactions with dissolved organic matter- Assessment of oxidant reactive moieties by optical measurements and the electron donating capacities. Water Res. 44, 64–75. https://doi.org/10.1016/j.watres.2018.06.059.

Page, S.E., Arnold, W.A., McNeill, K., 2010. Terephthalate as a probe for photochemically generated hydroxyl radical. J. Environ. Monit. 12, 1658–1665. https://doi.org/10.1039/C0EM00160K.

Pan, X.-M., Schuchmann, M.N., von Sonntag, C., 1993. Oxidation of benzene by the OH radical. A product and pulse radiolysis study in oxygenated aqueous solution. J. Chem. Soc. Perkin Trans. 2, 289–297. https://doi.org/10.1039/P29930000289.

Rabani, J., Mulac, W.A., Matheson, M.X., 1965. The pulse radiolysis of aqueous tetranitromethane . I. Rate constants and extinction coefficient of e-aq. II. Oxygenated solutions. J. Phys. Chem. 69, 53–70. https://doi.org/10.1021/j100885a011.

Rao, P.S., Hayon, E., 1975. Redox potentials of free radicals. IV. Superoxide and hydroperoxide radicals $^\bullet O_2^-$ and $^\bullet HO_2$. J. Phys. Chem. 79, 397–402. https://doi.org/10.1021/j100571a021.

Rebenne, L.M., González, A.C., Olson, T.M., 1996. Aqueous chlorination kinetics and mechanism of substituted dihydroxybenzenes. Environ. Sci. Technol. 30, 2235–2242. https://doi.org/10.1021/es950607t.

Rodier, J., Legube, B., Merlet, N., 2009. L'analyse de l'eau, 9 ed., p. 1600 Dunod.

Rodríguez, E.M., Márquez, G., Tena, M., Álvarez, P.M., Beltrán, F.J., 2015. Determination of main species involved in the first steps of TiO_2 photocatalytic degradation of organics with the use of scavengers: the case of ofloxacin. Appl. Catal. B Environ. 178, 44–53. https://doi.org/10.1016/j.apcatb.2014.11.002.

Ross, A.B., Bielski, B.H.J., Buxton, G.V., Cabelli, D.E., Helman, W.P., Huie, R.E., Grodkowski, J., Neta, P., Mulazzanin, Q.G., Wilkinson, F., 1998. NIST Standard Reference Database 40. NDRL/NIST Solution Kinetics Database: Version 3.0. Gaithersburg, MD. https://kinetics.nist.gov/solution/.

Santana-Casiano, J.M., González-Dávila, M., González, A.G., Millero, F.J., 2010. Fe(III) reduction in the presence of catechol in seawater. Aquat. Geochem. 16, 467–482. https://doi.org/10.1007/s10498-009-9088-x.

Schuchmann, M.N., von Sonntag, C., 1979. Hydroxyl radical-induced oxidation of 2-methyl-2-propanol in oxygenated solution. A product and pulse radiolysis

study. J. Phys. Chem. 83, 780–784. https://doi.org/10.1021/j100470a004.

Schuchmann, M.N., Bothe, E., von Sonntag, J., von Sonntag, C., 1998. Reaction of OH radicals with benzoquinone in aqueous solutions. A pulse radiolysis study. J. Chem. Soc., Perkin Trans. 2, 791–796. https://doi.org/10.1039/A708772A.

Schwarz, H.A., Bielski, B.H.J., 1986. Reactions of hydroperoxo and superoxide with iodine and bromine and the iodide (I_2^-) and iodine atom reduction potentials. J. Phys. Chem. 90, 1445–1448. https://doi.org/10.1021/j100398a045.

Sheng, Y., Abreu, I.A., Cabelli, D.E., Maroney, M.J., Miller, A.-F., Teixeira, M., Valentine, J.S., 2014. Superoxide dismutases and superoxide reductases. Chem. Rev. 114, 3854–3918. https://doi.org/10.1021/cr4005296.

Song, Y., Buettner, G.T., 2010. Thermodynamic and kinetic considerations for the reaction of semiquinone radicals to form superoxide and hydrogen peroxide. Free Radic. Biol. Med. 49, 919–962. https://doi.org/10.1016/j.freeradbiomed.2010.05.009.

U.S. EPA, 1996. Method 8315A (SW-846): Determination of Carbonyl Compounds by High Performance Liquid Chromatography (HPLC). Revision 1. Washington, DC.

von Gunten, U., 2018. Oxidation processes in water treatment: are we on track? Environ. Sci. Technol. 52, 5062–5075. https://doi.org/10.1021/acs.est.8b00586.

von Sonntag, C., von Gunten, U., 2012. Chemistry of Ozone in Water and Wastewater Treatment- from Basic Principles to Applications. IWA Publishing, London. https://doi.org/10.2166/9781780400839.

Walpen, N., Schroth, M.H., Sander, M., 2016. Quantification of phenolic antioxidant moieties in dissolved organic matter by flow-injection analysis with electrochemical detection. Environ. Sci. Technol. 50, 6423–6432. https://doi.org/10.1021/acs.est.6b01120.

Weishaar, J.L., Aiken, G.R., Bergamaschi, B.A., Fram, M.S., Fuji, R., Mopper, K., 2003. Evaluation of specific ultraviolet absorbance as an indicator of the chemical composition and reactivity of dissolved organic carbon. Environ. Sci. Technol. 37, 4702–4708. https://doi.org/10.1021/es030360x.

Wenk, J., von Gunten, U., Canonica, S., 2011. Effect of dissolved organic matter on the transformation of contaminants induced by excited triplet states and the hydroxyl radical. Environ. Sci. Technol. 45, 1334–1340. https://doi.org/10.1021/es102212t.

Wenk, J., Aeschbacher, M., Salhi, E., Canonica, S., von Gunten, U., Sander, M., 2013. Chemical oxidation of dissolved organic matter by chlorine dioxide, chlorine and ozone: effects on its optical and antioxidant properties. Environ. Sci. Technol. 47, 11147–11156. https://doi.org/10.1021/es402516b.

WHO, 1994. Environmental Health Criteria 157. Hydroquinone. World Health Organization, Geneva, Switzerland.

Yamazaki, I., Ohnishi, T., 1966. One-electron-transfer reactions in biochemical systems I. Kinetics analysis of the oxidation-reduction equilibrium between quinol-quinone and ferrro-ferricytochrome c. Biochim. Biophys. Acta 112, 469–481. https://doi.org/10.1016/0926-6585(66)90249-4.

Zehavi, D., Rabani, J., 1972. The oxidation of aqueous bromide ions by hydroxyl radicals. A pulse radiolytic investigation. J. Phys. Chem. 76, 312–319. https://doi.org/10.1021/j100647a006.